

NASA Contractor Report 3109

NASA  
CR  
3109  
c.1.

LOAN COPY: RETURN  
AFWL TECHNICAL LIBRARY  
KIRTLAND AFB, NM

TECH LIBRARY KAFB, NM  
0061909

# A Wave-Envelope Analysis of Sound Propagation in Nonuniform Circular Ducts With Compressible Mean Flows

A. H. Nayfeh, J. E. Kaiser,  
and B. S. Shaker

CONTRACT NAS1-13884  
MARCH 1979

**NASA**



NASA Contractor Report 3109

A Wave-Envelope Analysis  
of Sound Propagation in  
Nonuniform Circular Ducts  
With Compressible Mean Flows

A. H. Nayfeh, J. E. Kaiser,  
and B. S. Shaker  
*Virginia Polytechnic Institute & State University  
Blacksburg, Virginia*

Prepared for  
Langley Research Center  
under Contract NAS1-13884

**NASA**

National Aeronautics  
and Space Administration

**Scientific and Technical  
Information Office**

1979



## TABLE OF CONTENTS

	PAGE
1. INTRODUCTION.....	1
2. PROBLEM FORMULATION.....	8
3. METHOD OF SOLUTION.....	12
3.1 Critique of the Existing Methods.....	12
3.2 Form of Solution.....	14
3.3 Constraints.....	16
3.4 Equations Describing the Wave Envelopes.....	19
4. NUMERICAL SOLUTION.....	20
4.1 Mean-flow Model.....	20
4.2 Wall Admittance.....	22
4.3 Parallel-duct Eigenfunctions.....	22
4.4 Numerical Integration.....	23
4.5 Acoustic Pressure Profiles.....	24
4.6 Energy Flux.....	26
5. SAMPLE CASES.....	27
5.1 Definition of Input Variables for Program.....	27
5.2 Symmetry Checks.....	30
5.3 Comparison with one-dimensional theory.....	33
5.4 Comparison with Finite-Element Results.....	35
5.5 Straight Ducts with Variable Liners.....	37
5.6 General, Axisymmetric Case.....	38
5.7 Spinning Mode Case.....	39
5.8 Convergence of Results with Number of Modes.....	40
6. SUMMARY.....	43
APPENDIX A.....	45
FIGURES.....	48
REFERENCES.....	60

## 1. INTRODUCTION

The present practice of using high-bypass turbojet engines has resulted in a decrease in jet noise. However, these engines emit noise from their inlet nacelles above a desirable level. The present work is part of a considerable effort being made to reduce inlet noise.

One promising approach to the reduction of inlet noise is the use of a high subsonic Mach number inlet, or partially choked inlet, in conjunction with an acoustic duct liner. The use of choked inlets has long been recognized as an effective means of reducing upstream propagation although such inlets require careful design to prevent excessive losses in compressor performance. However, the physical mechanisms responsible for the noise reduction in high-subsonic Mach number inlets are not completely understood, and techniques for the theoretical analysis of sound propagation through regions of near-sonic mean flow are not available. Two major problems must be overcome in the development of such a model: (1) the mathematical techniques for the calculation of sound propagation in ducts are well-developed for parallel ducts but are not fully developed for ducts of varying cross section that carry mean flows with strong axial and transverse gradients; (2) linear acoustic equations are inadequate to describe acoustic propagation in regions of near-sonic mean flows<sup>1,2</sup>. In the investigation presented here, the first of these two problems was addressed, and a wave-envelope technique based on the method of variation of parameters was developed. This procedure can be used as the basis of the examination of the second aspect of the problem, the development of nonlinear models for the near-sonic region.

The concept of sound reduction by choked inlets has been investigated experimentally at great length. Several experimental investigators tested actual jet engines with various shapes of centerbodies as well as experimental ducts to choke the flow. Surveys of the concept of the choked inlet were given by Lumsdaine<sup>3</sup> and Klujber, et al<sup>4</sup>. An updated survey is presented here.

Sobell and Welliver<sup>5</sup> tested a Bristol Olympus 6 jet engine; the inlet of this engine was choked by using a sonic block silencer. Non-inlet noise radiation associated with this experiment may be a reason why only a 12 dB noise reduction was observed. Greatrex<sup>6</sup> conducted an experiment on an Avon engine with a bullet-shaped centerbody to choke the flow. He reported a 20 dB noise reduction.

To test the effect of choking the flow on the reduction of inlet noise, Sawhill<sup>7</sup> tested an ST model inlet with a translating centerbody and reported a 33 dB noise reduction when the throat Mach number of the inlet was increased from 0.63 to 0.9. Cawthorn, Morris, and Hayes<sup>8</sup> tested an SST inlet with a Viper 8 turbojet engine and a translating centerbody to choke the flow. They found that choking the flow resulted only in a 3 dB noise reduction. Using two centerbodies of different sizes to choke the flow of an SST inlet, Anderson<sup>9</sup> obtained a 20 dB noise reduction at a throat Mach number of 0.77. Anderson, et al<sup>10</sup> conducted a test on an airfoil grid inlet; they used two airfoils positioned in parallel in an inlet duct. They reported a loss of 7% in the inlet recovery pressure when they attained a 27 PNdB noise reduction.

Inlet guide vanes also have a significant effect on the noise reduction. Chestnutt and Stewart<sup>11</sup> conducted an experiment by using an accelerating inlet. They reported noise reductions up to 25 dB, due to the elimination of multiple pure tones, when the inlet approached choking conditions. The only drawback is that the noise reduction was accompanied by a significant reduction in the compressor efficiency. To determine the effect of the shape of the guide vane on the noise reduction, Chestnutt<sup>12</sup> tested uncambered and tapered inlet guide vanes. He obtained noise reductions of about 28 dB and 36 dB for the uncambered and tapered guide vanes, respectively. Anderson, et al<sup>10</sup> tested radial vane inlets and showed a 22.5 PNdB noise reduction with a 7% loss in recovery pressure.

Hawking and Lawson<sup>13</sup> reported a large reduction in acoustic energy for a waisted geometry. They suggested that this reduction is due to an increase in the axial Mach number. Benzakin, Kazin, and Savell<sup>14</sup>

conducted an experiment on a lined accelerating inlet. They concluded that the noise increases with increasing Mach number until throat Mach numbers of 0.6, then the noise level goes down with further increases in throat Mach number.

It is clear from the above experiments that inlet choking may be an effective noise suppression mechanism. The amount of noise reduction depends on how the choking is achieved. However, the choking may be accompanied by a loss in the compressor efficiency. Thus, the optimum choking configuration is the one accompanied by no loss or a minor loss in the compressor efficiency.

Many investigators studied the possibility of attaining a significant noise reduction with a minor loss in the compressor efficiency; they showed that the loss in the compressor efficiency can be minimized by carefully designing the centerbody.

Klujber<sup>15</sup> reported a noise reduction when a sonic inlet is used. This reduction occurs when the average throat Mach number increases from 0.5 to 1.0. He reported also that more reduction of the noise can be attained but with a further decrease in the inlet recovery pressure.

Higgins, Smith, and Wise<sup>16</sup> measured a significant noise reduction with a moderate loss in recovery pressure by using variable cowl inlets. Koch, Ciskowski, and Garzon<sup>17</sup> reported a 15 dB sound level attenuation with a minimum loss of aerodynamic performance when operating at an average Mach number of 0.79. Miller and Abbott<sup>18</sup> tested experimentally an inlet with a translating centerbody to choke the flow; they reported a 20 dB noise reduction with a pressure recovery of 98.5%. Abbott<sup>19</sup> indicated that the most efficient method to achieve aerodynamic performance and noise reduction is to use a cylindrical centerbody at takeoff and a bulbshaped centerbody at approach to choke the flow. He reported that increasing the inlet length results in a higher recovery pressure for a given noise reduction. Groth<sup>20</sup> tested a J-85 turbojet engine using a translating centerbody inlet with a radial vane. He measured a 40 dB reduction in a fully-choked inlet while maintaining a recovery pressure of 92.1%. Savkar and Kazin<sup>21</sup> showed that a 99% recovery pressure can be attained for the same amount of noise reduction

by proper contouring of the centerbody and careful designing of the diffuser. Miller<sup>22</sup> experimentally determined how a sonic inlet can be designed to have a significant noise reduction with a minimum loss of total pressure.

As we see above, most, but not all, of these investigations have noted significant reductions of the noise level when the inlet is choked. The geometry of the inlet, the geometry of the centerbody and the operating condition seem to have an effect on the acoustic as well as on the aerodynamic performance. Further, most of the potential noise reduction is achieved by operating in the partially choked state (mean Mach number in the throat of 0.8-0.9). Some investigators (e.g., Chestnutt and Clark<sup>23</sup> and Sobel and Welliver<sup>5</sup>) report the possibility of substantial "leakage" through the wall boundary layers, whereas others (e.g. Klujber<sup>15</sup>) report that such leakage is minor. Although the experimental studies have demonstrated that the choked inlet is a viable technique, they have not provided insight into the physical mechanisms that are responsible for the noise reduction or that explain the differences among the several experimental results.

Several analytical as well as numerical techniques have been developed for the analysis of wave propagation in uniform and nonuniform ducts. Surveys of these techniques were made by Nayfeh, Kaiser, and Telionis<sup>24</sup>, Nayfeh<sup>25</sup>, and Vaidya and Dean<sup>26</sup>. In this study, only a short critique is presented.

The problem of sound propagation in a uniform duct (rectangular, circular, etc.), with or without mean flows, for hard as well as lined walled ducts, has been studied extensively. A number of parametric studies have been done for the case of uniform ducts, showing the effect of each parameter on noise attenuation. A large number of papers are cited in the review article of Nayfeh, et al<sup>24</sup>, each of which discusses at least one of the acoustic parameters.

The investigation of the problem of sound propagation in nonuniform ducts was motivated by the experimental discoveries discussed earlier in this introduction. These investigations are discussed below in order of increasing complexity of the mean flow: no flow, one-dimensional flow, and two-dimensional flow.

The problem of sound propagation in a variable-area duct with no-mean flow was discussed for horns by Webster<sup>27</sup>. He considered only the lowest propagating mode. Stevenson<sup>28</sup> extended Webster's work to investigate the propagation of various modes. He used the method of weighted residuals to solve the problem of wave propagation in hard-walled horns of arbitrary shape. Eversman, Cook, and Beckemeyer<sup>29</sup> extended the method of weighted residuals to study multimodal propagation in a non-uniform lined duct.

Alfredson<sup>30</sup> divided the variable area duct into a finite number of stepped uniform ducts. Thus, a large number of stepped uniform ducts are needed to provide sufficient accuracy for cases with large axial gradients.

Nayfeh and Telionis<sup>31</sup> used the method of multiple scales to analyze wave propagation in ducts with slowly, but arbitrarily, varying cross sections and wall admittance. For the case of hard-walled ducts, the solution of Nayfeh and Telionis is equivalent to that of Stevenson for slowly-varying ducts. Nayfeh and Telionis pointed out that both of the solutions breakdown near cut-off; they suggested using a turning point analysis (see 7.3.2 of reference 32) to overcome this problem.

Isakovitch<sup>33</sup>, Samuels<sup>34</sup>, and Salant<sup>35</sup> obtained perturbation solutions for wave propagation in ducts whose rigid walls have sinusoidal undulations of small amplitudes. Their perturbation expansions are not valid near resonance conditions; that is, whenever the wave number of the wall undulation is approximately equal to the sum or difference of the wave numbers of any two acoustic modes. Nayfeh<sup>36,37</sup> and Nayfeh and Kandil<sup>38</sup> used the method of multiple scales to obtain an expansion valid near resonance. They found that neither of the modes involved in the resonance can propagate in the duct without exciting the other. Moreover, they found that coupling of an upstream and a downstream mode may lead to their being cutoff.

Quinn<sup>39</sup> and Baumeister and Rice<sup>40</sup> developed finite-difference methods to study a plane wave propagating in nonuniform ducts. We note that a large amount of computation will be required with these purely numerical techniques because a large number of grid points are needed to

provide sufficient accuracy. The axial step must be small enough to resolve the smallest wave length, while the transverse step must be small enough to resolve the highest mode. Thus, the computational time increases rapidly with increasing frequency and duct length. To reduce the computational time for plane waves in a two-dimensional duct, Baumeister<sup>41</sup> expressed the potential function  $\phi(x,y,t)$  as  $\psi(x,y) \exp[i(kx - \omega t)]$ , where  $k$  is a properly chosen constant, such as the wavenumber in a hard-walled duct. Then he solved for  $\psi(x,y)$  using finite differences.

Approximating the mean flow by a quasi-one-dimensional flow, Powell<sup>42</sup> used a multiple reflection method to study the acoustic propagation through variable-area ducts. Eisenberg and Kao<sup>43</sup> analyzed plane waves in a specially-chosen variable-area duct that yields an equation with constant coefficients. Davis and Johnson<sup>44</sup> used a forward-integration technique to solve the acoustic equation describing the axial variations. Huerre and Karamcheti<sup>45</sup> analyzed the propagation of the lowest mode by using the WKB approximation, while King and Karamcheti<sup>46</sup> developed a second-order-accurate numerical method to solve for the propagation through a variable-area duct by using the method of characteristics.

Nayfeh and co-workers studied extensively the propagation of various acoustic modes in ducts having slowly-varying cross sections and carrying general mean flows. Nayfeh, Telionis, and Lekoudis<sup>47</sup> discussed the acoustic propagation in lined plane ducts with varying cross sections and sheared mean flow. This work was extended to annular ducts by Nayfeh, Kaiser, and Telionis<sup>48</sup>. The effect of a compressible, sheared mean flow on sound transmission through a variable-area plane duct was studied by Nayfeh and Kaiser<sup>49</sup>. Using their method, one can determine the transmission and attenuation of all modes including the effect of transverse as well as axial gradients, but the technique is limited to slow variations. Moreover, the expansion needs to be carried out to second order in order to determine reflection and intermodal coupling of the acoustic signal. Nayfeh, Kaiser, Marshall and Hurst<sup>50</sup> carried out an experimental study of sound propagating in variable-area ducts with and without mean flows. Hard as well as lined duct walls were used. The axial variations were small. The experimental data are in reasonable agreement with the multiple-scales solution.

Eversman<sup>51</sup> developed a theory by using the method of weighted residuals to determine the transmission of sound in plane nonuniform hard-walled ducts with mean flow. He obtained equations describing the axial variations of the modes. To solve these equations, one needs a large number of axial steps, especially as the mean Mach number approaches unity and the frequency becomes large, leading to a rapid decrease in the axial wavelength.

In summary, purely numerical techniques suffer from the requirement of large computation times, and they have been restricted thus far to cases of no-mean flow. (During the period of time that the work reported here and in an earlier report<sup>52</sup> was being carried out, finite-element methods for ducts with compressible mean flows were developed by Sigman, Majjigi and Zinn<sup>53</sup> and by Abrahamson<sup>54</sup>). Analytical techniques have only been applied thus far to simple cases of one-dimensional mean flows and/or plane acoustic waves and/or slowly-varying duct geometry and promise to become unwieldy for more general cases. Thus, the specific analytical and computational tools that are needed for the study of wave propagation in ducts involving large gradients in both axial and transverse directions are lacking.

In this study an acoustic theory is developed to determine the sound transmission and attenuation through an infinite, hard-walled or lined circular duct carrying compressible, sheared mean flows and having a variable cross section. The theory is applicable to large as well as small axial variations, as long as the mean flow does not separate. The technique is based on solving for the envelopes of the quasi-parallel acoustic modes that exist in the duct instead of solving for the actual wave. The feasibility of this technique has been demonstrated by Kaiser and Nayfeh<sup>55</sup> for plane ducts with no-mean flow.

The problem is formulated in the following section, the method of solution is presented in Section 3, the numerical solution is described in Section 4, the numerical results and discussion are presented in Section 5, and the conclusions are presented in Section 6.

## 2. PROBLEM FORMULATION

The transmission and attenuation of sound in hard- and soft-walled circular inlet ducts (Figure 1) carrying viscous or inviscid high subsonic mean flows is examined. The mean Mach number in the throat is near sonic; thus, the axial and radial gradients of the mean flow can be large. The cross section of the duct varies arbitrarily with the axial distance.

The symbols used in the analysis are listed in Appendix A, except for a few which are used only where they are defined. All symbols are nondimensional unless specifically noted otherwise. Velocities, lengths, and time are made dimensionless by using the reference speed of sound  $c_a^*$  (value in mean flow at  $x = 0$  and  $r = 0$ ), the radius  $R_0^*$  of the duct in the uniform region (Figure 1), and  $R_0^*/c_a^*$ , respectively. The pressure  $p$  is made dimensionless by using  $\rho_a^* c_a^{*2}$ , the density  $\rho$  and temperature  $T$  are made dimensionless by using their corresponding reference values, while the viscosity  $\mu$  and the thermal conductivity  $\kappa$  are made dimensionless by using their wall values in the uniform section. In terms of these dimensionless variables, the equations which describe the unsteady viscous flow in a duct are (see for example, Schlichting<sup>56</sup>).

conservation of mass

$$\frac{\partial \rho}{\partial t} + \nabla \cdot (\rho \vec{V}) = 0 \quad (1)$$

conservation of momentum

$$\rho \left( \frac{\partial \vec{V}}{\partial t} + \vec{V} \cdot \nabla \vec{V} \right) = - \nabla p + \frac{1}{Re} \nabla \cdot \underline{\underline{\tau}} \quad (2)$$

conservation of energy

$$\begin{aligned} \rho \left( \frac{\partial T}{\partial t} + \vec{V} \cdot \nabla T \right) - (\gamma - 1) \left( \frac{\partial p}{\partial t} + \vec{V} \cdot \nabla p \right) \\ = \frac{1}{Re} \left[ \frac{1}{Pr} \nabla \cdot (\kappa \nabla T) + (\gamma - 1) \Phi \right] \end{aligned} \quad (3)$$

equation of state

For a perfect gas,

$$\gamma p = \rho T \quad (4)$$

For a Newtonian fluid, the dimensionless viscous-stress tensor  $\underline{\tau}$  and the dimensionless dissipation function  $\Phi$  are related to  $\vec{v}$  by

$$\underline{\tau} = \mu[\nabla\vec{v} + (\nabla\vec{v})^T] + \lambda\nabla \cdot \vec{v}$$

$$\Phi = \underline{\tau} : \nabla\vec{v} = \sum_{j=1}^3 \sum_{i=1}^3 \tau_{ij} \partial v_i / \partial x_j$$

where  $(\nabla\vec{v})^T$  denotes the transpose of  $\nabla\vec{v}$ .

In general, the ducts carry a high subsonic, steady, sheared mean flow that satisfies equations (1) through (4). The presence of sound in the ducts results in the perturbation of the flow quantities so that

$$q(\vec{r}, t) = q_0(\vec{r}) + q_1(\vec{r}, t) \quad (5)$$

where  $q$  stands for any flow quantity,  $q_0$  is the mean-flow part, and  $q_1$  is the acoustic part. Substituting equation (5) into equations (1) through (4) and eliminating the mean-flow quantities, one obtains the following acoustic equations:

$$\frac{\partial \rho_1}{\partial t} + \nabla \cdot (\rho_0 \vec{v}_0 + \rho_1 \vec{v}_0) = NL \quad (6)$$

$$\rho_0 \left( \frac{\partial \vec{v}_1}{\partial t} + \vec{v}_0 \cdot \nabla \vec{v}_1 + \vec{v}_1 \cdot \nabla \vec{v}_0 \right) + \rho_1 \vec{v}_0 \cdot \nabla \vec{v}_0 =$$

$$- \nabla p_1 + \frac{1}{Re} \nabla \cdot \underline{\tau}_1 + NL \quad (7)$$

$$\rho_0 \left( \frac{\partial T}{\partial t} + \vec{v}_0 \cdot \nabla T_1 + \vec{v}_1 \cdot \nabla T_0 \right) + \rho_1 \vec{v}_0 \cdot \nabla T_0 - (\gamma - 1) \left( \frac{\partial p_1}{\partial t} \right.$$

$$+ \vec{v}_0 \cdot \nabla p_1 + \vec{v}_1 \cdot \nabla p_0 \left. \right) = \frac{1}{Re} \left[ \frac{1}{Pr} \nabla \cdot (\kappa_0 \nabla T_1 + \kappa_1 \nabla T_0) \right.$$

$$\left. + (\gamma - 1) \Phi_1 \right] + NL \quad (8)$$

$$\frac{p_1}{p_0} = \frac{\rho_1}{\rho_0} + \frac{T_1}{T_0} \quad (9)$$

where  $\underline{\tau}_1$  and  $\Phi_1$  are linear in the acoustic quantities and NL stands for the nonlinear terms in the acoustic quantities.

No solution to equations (6) through (9) subject to general initial and boundary conditions is available yet. To determine solutions for the propagation of sound in ducts, researchers have used simplifying assumptions. Here, the nonlinear and viscous terms in the acoustic

equations are neglected, and the mean flow is taken to be a function of the axial and radial coordinates only. Further, we neglect swirling mean flows. The assumption of linearization is not valid for high sound-pressure levels. The effects of the nonlinear acoustic properties of the lining material become significant when the sound-pressure level exceeds about 130 dB (re 0.0002 dyne/cm<sup>2</sup>), while the effects of the gas nonlinearity become significant when the sound pressure level exceeds about 160 dB. In particular, the nonlinearity of the gas must be included when the mean flow is transonic (i.e., near the throat<sup>1,2</sup>). Nayfeh<sup>57</sup> showed that the viscous terms in the acoustic equations produce an effective admittance at the wall that leads to small dispersion and attenuation. For lined ducts, this admittance produced by the acoustic boundary layer may be neglected, but it cannot be neglected for hard-walled ducts, as demonstrated analytically and experimentally by Pestorius and Blackstock<sup>58</sup>.

A cylindrical coordinate system  $(r, \theta, x)$  is introduced as shown in Figure 1. Since there is no swirling flow, each flow quantity  $q_1(r, x, \theta, t)$  can be expressed, for sinusoidal time variations, as

$$q_1(r, x, \theta, t) = \sum_{m=0}^{\infty} q_{1m}(r, x) \exp[-i(\omega t - m\theta)] \quad (10)$$

where  $\omega$  is the dimensionless frequency. Using the above assumptions, one can rewrite equations (6) through (9) in cylindrical coordinates as

$$-i\omega\rho_1 + \frac{\partial}{\partial x} (\rho_0 u_1 + u_0 \rho_1) + \frac{i\rho_0 m}{r} w_1 + \frac{1}{r} \frac{\partial}{\partial r} (r\rho_0 v_1 + r v_0 \rho_1) = 0 \quad (11)$$

$$\begin{aligned} \rho_0 [-i\omega u_1 + \frac{\partial}{\partial x} (u_0 u_1) + v_0 \frac{\partial u_1}{\partial r} + v_1 \frac{\partial u_0}{\partial r}] + \rho_1 [u_0 \frac{\partial u_0}{\partial x} + \\ + v_0 \frac{\partial u_0}{\partial r}] = - \frac{\partial p_1}{\partial x} \end{aligned} \quad (12)$$

$$\begin{aligned} \rho_0 [-i\omega v_1 + \frac{\partial}{\partial r} (v_0 v_1) + u_0 \frac{\partial v_1}{\partial x} + u_1 \frac{\partial v_0}{\partial x}] + \rho_1 [v_0 \frac{\partial v_0}{\partial r} + u_0 \frac{\partial v_0}{\partial x}] \\ = - \frac{\partial p_1}{\partial r} \end{aligned} \quad (13)$$

$$\rho_0 [-i\omega w_1 + v_0 \frac{\partial w_1}{\partial r} + \frac{v_0 w_1}{r} + u_0 \frac{\partial w_1}{\partial x}] = - \frac{im}{r} p_1 \quad (14)$$

$$\begin{aligned}
& \rho_0[-i\omega T_1 + v_0 \frac{\partial T_1}{\partial r} + u_0 \frac{\partial T_1}{\partial x} + v_1 \frac{\partial T_0}{\partial r} + u_1 \frac{\partial T_0}{\partial x}] + \rho_1[v_0 \frac{\partial T_0}{\partial r} \\
& + u_0 \frac{\partial T_0}{\partial x}] - (\gamma-1)[-i\omega p_1 + u_0 \frac{\partial p_1}{\partial x} + v_0 \frac{\partial p_1}{\partial r} + u_1 \frac{\partial p_0}{\partial x} \\
& + v_1 \frac{\partial p_0}{\partial r}] = 0
\end{aligned} \tag{15}$$

$$\frac{p_1}{p_0} = \frac{\rho_1}{\rho_0} + \frac{T_1}{T_0} \tag{16}$$

where  $u, v$ , and  $w$  are the velocities in the axial, radial, and azimuthal directions, respectively, and the subscript  $m$  has been suppressed.

To complete the problem formulation, one needs to specify the initial and boundary conditions. The boundary conditions are based on the assumption that the duct wall is lined with a point-reacting acoustic material whose specific acoustic admittance  $\beta$  may vary along the duct. For no-slip mean flows, a requirement of continuity of the particle displacement gives

$$v_1 - R'u_1 = \frac{\beta}{\rho_w c_w} p_1 \sqrt{1 + r'^2} \quad \text{at } r = R \tag{17}$$

where  $R'$  is the slope of the wall and the subscript  $w$  refers to values at the wall. The final results are desired in the form of transmission and reflection matrices<sup>59</sup> for a given duct section; thus the initial conditions consist of the successive input of each acoustic mode at the duct entrance.

### 3. METHOD OF SOLUTION

#### 3.1 Critique of the Existing Methods

Since there is no exact solution available yet for equations (11) through (17) in ducts of varying cross sections, a number of approaches have been developed to determine approximate solutions to this problem<sup>24,25</sup>. These approaches include quasi-one-dimensional approximations, solutions for slowly-varying cross sections, solutions for weak wall undulations, variational methods, approximation of the duct by a series of stepped uniform cross sections, and finite-difference and finite-element methods. A short critique of these approaches is included next (more detailed critiques are given in references 24 and 25), and it is followed by the proposed acoustic wave-envelope technique.

In the quasi-one-dimensional approach, one can determine only the lowest mode in ducts with slowly-varying cross sections and cannot account for transverse mean-flow gradients or large wall admittance.

In the slowly-varying cross-section approach, one can determine the transmission and attenuation for all modes including the effects of transverse as well as axial gradients, but the technique is limited to slow variations and the expansion needs to be carried out to second order to determine reflections of the acoustic signal.

In the weak wall-undulation approach, one assumes that the dimensionless duct radius is described by  $R = 1 + \epsilon R_1(x)$ , where  $\epsilon$  is small. Thus, in this approach one can account for all effects except large axial variations.

In the variational approach, one uses either the Rayleigh-Ritz procedure, which requires knowledge of the Lagrangian describing the problem, or the Galerkin procedure (the method of weighted residuals). Since the Lagrangian is not known yet for the general problem, the Galerkin procedure is the only applicable technique at this time. According to this procedure, one chooses basis functions (usually the mode shapes of a quasi-parallel problem) and represents the pressure, for example, as

$$p_1 = \sum_{n=1}^{\infty} p_n(x)\psi_n(r,x) \quad (18)$$

where the  $\psi_n$  are the basis functions which, in general, do not satisfy the boundary conditions. On expanding all flow variables in the form of equation (18), substituting the result into equations (11) through (17), and using the Galerkin procedure to minimize the error, one obtains differential equations describing the  $p_n$ . Since the  $\psi_n$  do not satisfy the equations and the boundary conditions, a large number of terms are needed to satisfy the equations and the boundary conditions and hence represent the solution for large cross-sectional variations; this leads to serious convergence questions. These problems can be minimized by choosing the  $\psi_n$  to be the quasi-parallel mode shapes corresponding to the propagation coefficients  $k_n$ . The functions  $p_n(x)$  vary rapidly even for a uniform duct:  $p_n(x) \propto \exp(ik_n x)$ , and  $k_n$  can be very large for high frequency, low-order modes. Thus, small axial steps must be used in the computations, resulting in a large computation time, which increases very rapidly with axial distance and sound frequency.

In approximating a duct with a continuously-varying cross-sectional area by a series of stepped uniform ducts, a large number of uniform segments are needed to provide sufficient accuracy for the solution when the axial gradients are large. Thus, this approach is impractical in the present problem because an enormous amount of computation time is needed even for the case of a moderate number of uniform segments.

This short discussion shows that the above techniques would certainly either fail to produce sufficient accuracy for the present problem or would require large computation times. Thus, alternate techniques must be developed. The procedure to be developed has the further requirement that it be capable of calculating the transmission and reflection coefficients of the duct modes in order that the results be compatible with the general approach developed by Zorumski<sup>59</sup>. The generation of transmission and reflection coefficients require repetitive calculations through the duct as each mode is considered successively as input to the duct. For each such calculation, it is necessary to use very small axial and radial steps to represent the rapidly-varying mode shapes and the axial oscillations of each mode. (In fact,

a computational difficulty exists in calculating the higher-order Bessel functions that represent the mode shapes in a uniform duct carrying uniform mean flow unless asymptotic expansions are used.) The axial step must be much smaller than the wavelength of the lowest mode in order to be able to determine the axial variations. These small steps could cause the error in the numerical solution to increase very rapidly with axial distance. Thus purely numerical methods would be impractical because of the excessive amount of computation time. Similar problems have been encountered by astronomers who developed what is usually called the special perturbation method in which one solves only for the wave envelope instead of solving for the wave itself. Here we use this idea to develop a wave-envelope technique for solving the present problem.

### 3.2 Form of Solution

With this approach, one uses the method of variation of parameters to change the dependent variables from the fast-varying variables to others that vary slowly. Moreover, the solution is approximated by a finite sum of the quasi-parallel-duct eigenfunctions.

Thus, we seek an approximate solution to equations (11) through (17) in the form

$$p_1 \approx \sum_{n=1}^N \left\{ A_n(x) \psi_n^p(r,x) \exp(i \int k_n(x) dx) + \tilde{A}_n(x) \tilde{\psi}_n^p(r,x) \times \right. \\ \left. \exp(i \int \tilde{k}_n(x) dx) \right\} \quad (19)$$

$$u_1 \approx \sum_{n=1}^N \left\{ A_n(x) \psi_n^u(r,x) \exp(i \int k_n(x) dx) + \tilde{A}_n(x) \tilde{\psi}_n^u(r,x) \times \right. \\ \left. \exp(i \int \tilde{k}_n(x) dx) \right\} \quad (20)$$

with similar expressions for  $v_1$ ,  $w_1$ ,  $T_1$ , and  $\rho_1$ , where the tilde refers to upstream propagation, the  $\psi_n(r,x)$  are the quasi-parallel mode shapes corresponding to the quasi-parallel propagation coefficients  $k_n(x)$ , and the  $A_n(x)$  are complex functions whose moduli and arguments represent, in some sense, the amplitudes and the phases of the  $(m,n)$  modes. The

circumferential mode number  $m$  is assumed to be specified and the corresponding subscript on  $A$ ,  $\psi$ , and  $k$  is not explicitly stated; each variable is expressed as a summation over a finite number of radial modes  $N$ , with  $n = 1$  denoting the fundamental radial mode rather than the conventional  $n = 0$ . Since  $k_n$  is complex, the exponential factor contains an estimate of the attenuation of the  $(m,n)$  mode. Thus, the envelope of the  $(m,n)$  mode is given by

$$|A_n(x)| \exp[-\int \alpha_n(x) dx]$$

where  $\alpha_n$  is the imaginary part of  $k_n$ .

Since the  $\psi_n$  are the quasi-parallel mode shapes, they are the solutions of the following problem:

$$-i\hat{\omega}\psi^p + ik\rho_0\psi^u + \frac{i\rho_0 m}{r}\psi^w + \frac{1}{r}\frac{\partial}{\partial r}(r\rho_0\psi^v) = 0 \quad (21)$$

$$-i\rho_0\hat{\omega}\psi^u + \rho_0\frac{\partial u_0}{\partial r}\psi^v + ik\psi^p = 0 \quad (22)$$

$$-i\rho_0\hat{\omega}\psi^v + \frac{\partial\psi^p}{\partial r} = 0 \quad (23)$$

$$-i\rho_0\hat{\omega}\psi^w + \frac{im}{r}\psi^p = 0 \quad (24)$$

$$-i\rho_0\hat{\omega}\psi^T + \rho_0\frac{\partial T_0}{\partial r}\psi^v + i(\gamma-1)\hat{\omega}\psi^p = 0 \quad (25)$$

$$\frac{\psi^p}{\rho_0} = \frac{\psi^u}{\rho_0} + \frac{\psi^T}{T_0} \quad (26)$$

$$\psi^v - \frac{\beta}{\rho_w c_w}\psi^p = 0 \text{ at } r = R \quad (27)$$

where

$$\hat{\omega} = \omega - ku_0 \quad (28)$$

Equation (21) - (28) can be combined to yield the following problem<sup>57</sup> for  $\psi^p$ :

$$\frac{\partial^2\psi^p}{\partial r^2} + \left[\frac{1}{r} + \frac{T_0'}{T_0} + \frac{2ku_0'}{\hat{\omega}}\right]\frac{\partial\psi^p}{\partial r} + \left[\frac{\hat{\omega}^2}{T_0} - k^2 - \frac{m^2}{r^2}\right]\psi^p = 0 \quad (29)$$

$$\frac{\partial\psi^p}{\partial r} - i\frac{\omega\beta}{T_w/2}\psi^p = 0 \text{ at } r = R \quad (30)$$

At each axial location, the solution of equations (29) and (30) yields  $\psi_n^p(r;x)$  and its corresponding propagation coefficient  $k_n(x)$ . Since the basis functions  $\psi_n^p(r;x)$  vary in the axial direction, they must be normalized in some manner to provide significance to the axial variations of the mode amplitudes. The normalization used in this study is the same as that defined by Zorumski<sup>59</sup>:

$$\int_0^R r[\psi_n^p(r;x)]^2 dr = 1$$

Then, equations (21) - (26) are used to express the mode shapes of the other flow variables in terms of  $\psi_n^p$  and  $k_n$ .

### 3.3 Constraints

Since the transverse dependence in the assumed solution, equations (19) and (20), is chosen a priori, it cannot satisfy equations (11) - (17) exactly. Thus, the assumed solution must be subjected to constraints. Rather than using the usual method of weighted residuals which forces the residuals in each of the basic equations (11) - (16) and the boundary condition (17) to be orthogonal to some a priori chosen functions, we require the deviations from the quasi-parallel solution to be orthogonal to every solution of the adjoint quasi-parallel problem. This approach assures the recovery of the results of the method of multiple scales<sup>32</sup> when the axial variations are slow<sup>55</sup>.

To enforce the constraints, one must define the problem adjoint to the quasi-parallel problem. To this end, one can multiply equations (21) - (26) by the functions  $\phi_1, \phi_2, \phi_3, \phi_4, \phi_5,$  and  $\phi_6$ , respectively, where the  $\phi_n(r,x)$  are solutions of the adjoint problem, add the resulting equations, integrate the result by parts from  $r = 0$  to  $r = R$  thereby transferring the  $r$ -derivatives from the  $\psi$ 's to the  $\phi$ 's, and obtain

$$\begin{aligned} & \int_0^R \psi^p [-i\hat{\omega}\phi_1 - \phi_6/\rho_0] dr + \int_0^R i\rho_0\psi^u [-\hat{\omega}\phi_2 + k\phi_1] dr + \int_0^R \rho_0\psi^v [-i\hat{\omega}\phi_3 \\ & + \frac{\partial u_0}{\partial r} \phi_2 - r \frac{\partial}{\partial r} \left( \frac{\phi_1}{r} \right) + \frac{\partial T_0}{\partial r} \phi_5] dr + \int_0^R i\rho_0\psi^w [-\hat{\omega}\phi_4 \\ & + \frac{m}{r} \phi_1] dr + \int_0^R \psi^p [ik\phi_2 - \frac{\partial \phi_3}{\partial r} + \frac{im}{r} \phi_4 + i(\gamma-1)\hat{\omega}\phi_5 \\ & + \phi_6/p_0] dr + \int_0^R \rho_0\psi^T [-i\hat{\omega}\phi_5 - p_0\phi_6] dr + [\rho_0\psi^v \phi_1 + \psi^p \phi_3]_0^R = 0 \end{aligned} \quad (31)$$

Then, the adjoint equations are obtained by setting each of the bracketed terms in the integrands of equation (31) to zero; that is

$$\hat{i}\omega\phi_1 + \phi_6/\rho_0 = 0 \quad (32)$$

$$-\hat{\omega}\phi_2 + k\phi_1 = 0 \quad (33)$$

$$-\hat{i}\omega\phi_3 + \frac{\partial u_0}{\partial r}\phi_2 - r\frac{\partial}{\partial r}\left(\frac{\phi_1}{r}\right) + \frac{\partial T_0}{\partial r}\phi_5 = 0 \quad (34)$$

$$-\hat{\omega}\phi_4 + \frac{m}{r}\phi_1 = 0 \quad (35)$$

$$ik\phi_2 - \frac{\partial\phi_3}{\partial r} + \frac{im}{r}\phi_4 + i(\gamma-1)\hat{\omega}\phi_5 + \phi_6/\rho_0 = 0 \quad (36)$$

$$\rho_0\hat{i}\omega\phi_5 + \phi_6/T_0 = 0 \quad (37)$$

Equation (31) is reduced to

$$(\rho_0\psi^V\phi_1 + \psi^P\phi_3)_{r=0} = (\rho_0\psi^V\phi_1 + \psi^P\phi_3)_{r=R} \quad (38)$$

From equations (32) - (35) and (37), one can express each of the  $\phi_n$  as a function of  $\phi_1$ :

$$\phi_2 = \frac{k}{\hat{\omega}}\phi_1 \quad (39)$$

$$\phi_3 = \frac{irT_0}{\hat{\omega}^2}\frac{\partial}{\partial r}\left(\frac{\hat{\omega}\phi_1}{rT_0}\right) \quad (40)$$

$$\phi_4 = \frac{m\phi_1}{r\hat{\omega}} \quad (41)$$

$$\phi_5 = \frac{\phi_1}{T_0} \quad (42)$$

$$\phi_6 = -i\rho_0\hat{\omega}\phi_1 \quad (43)$$

Using equations (39)-(43) in equation (36), one then obtains the governing equation for  $\phi_1$ :

$$\frac{1}{r}\frac{\partial}{\partial r}\left[\frac{rT_0}{\hat{\omega}^2}\frac{\partial\eta}{\partial r}\right] + \left[1 - \frac{T_0k^2}{\hat{\omega}^2} - \frac{T_0m^2}{r^2\hat{\omega}^2}\right]\eta = 0 \quad (44)$$

where

$$\eta = \frac{\phi_1\hat{\omega}}{rT_0} \quad (45)$$

It can be shown easily that equations (29) and (44) are the same; thus  $\eta$  and  $\psi^P$  satisfy the same differential equation. The boundary conditions on  $\eta$  are obtained from equation (38) by substitution for  $\psi^V$  from equation (23), for  $\phi_3$  from equation (40), and for  $\phi_1$  from equation (45). The result is

$$\frac{irT_0}{\omega^2} \left[ -\frac{\partial \psi^P}{\partial r} \eta + \psi^P \frac{\partial \eta}{\partial r} \right]_{r=R} = \frac{irT_0}{\omega^2} \left[ -\frac{\partial \psi^P}{\partial r} \eta + \psi^P \frac{\partial \eta}{\partial r} \right]_{r=0} \quad (46)$$

If one requires that  $\eta$  be bounded at  $r = 0$ , just as  $\psi^P$  is, then the right-hand side vanishes. Using equation (30) to eliminate  $\partial \psi^P / \partial r$  and noting that  $\psi^P$  is arbitrary at  $r = R$ , one obtains

$$\frac{\partial \eta}{\partial r} - \frac{i\omega\beta}{T_1/2} \eta = 0 \quad \text{at } r = R \quad (47)$$

Since the boundary condition (47) is the same as the boundary condition (30), one can set  $\eta = \psi^P$  without loss of generality, and hence one does not need to solve the adjoint problem. One needs only to solve the quasi-parallel problem to determine  $\psi_n^P$  and then determine  $\phi_{1n}$  from

$$\phi_{1n} = \frac{rT_0\psi_n^P}{\omega} \quad (48)$$

according to equation (45). The remaining  $\phi$ 's are then determined from equations (39)-(43).

Once the adjoint functions are known, the constraint conditions are determined as follows. On multiplying equations (11)-(16) by  $\phi_{1n}, \phi_{2n}, \dots, \phi_{6n}$ , respectively, adding the resulting equations, integrating the result by parts from  $r = 0$  to  $r = R$  to transfer the  $r$ -derivatives to the  $\phi$ 's, and using equations (32)-(37) and (17), one obtains the following constraint:

$$\int_0^R \left\{ \begin{aligned} &\phi_{1n} [-iu_0 k_n \rho_1 - ik_n \rho_0 u_1 + \frac{\partial}{\partial x} (\rho_0 u_1 + u_0 \rho_1)] - rv_0 \rho_1 \frac{\partial}{\partial r} \left( \frac{\phi_{1n}}{r} \right) \\ &+ \phi_{2n} [-iu_0 k_n \rho_0 u_1 - ik_n p_1 + \rho_0 \frac{\partial (u_0 u_1)}{\partial x} + \rho_1 (u_0 \frac{\partial u_0}{\partial x} + v_0 \frac{\partial u_0}{\partial r}) \\ &+ \frac{\partial p_1}{\partial x}] - u_1 \frac{\partial}{\partial r} (\rho_0 v_0 \phi_{2n}) + \phi_{3n} [-iu_0 k_n \rho_0 v_1 + \rho_0 u_0 \frac{\partial v_1}{\partial x} \\ &+ \rho_0 u_1 \frac{\partial v_0}{\partial x} + \rho_1 (v_0 \frac{\partial v_0}{\partial r} + u_0 \frac{\partial v_0}{\partial x})] - v_0 v_1 \frac{\partial}{\partial r} (\rho_0 \phi_{3n}) \\ &+ \phi_{4n} [-ik_n \rho_0 u_0 w_1 + \frac{\rho_0 v_0 w_1}{r} + \rho_0 u_0 \frac{\partial w_1}{\partial x}] - w_1 \frac{\partial}{\partial r} (\rho_0 v_0 \phi_{4n}) \\ &+ \phi_{5n} [-iu_0 k_n \rho_0 T_1 + (\gamma-1)iu_0 k_n p_1 + \rho_0 u_0 \frac{\partial T_1}{\partial x} + \rho_0 u_1 \frac{\partial T_0}{\partial x} + \rho_1 (v_0 \frac{\partial T_0}{\partial r} \\ &+ u_0 \frac{\partial T_0}{\partial x}) - (\gamma-1)(u_0 \frac{\partial p_1}{\partial x} + u_1 \frac{\partial p_0}{\partial x} + v_1 \frac{\partial p_0}{\partial r})] - T_1 \frac{\partial}{\partial r} (\rho_0 v_0 \phi_{5n}) \\ &+ (\gamma-1)p_1 \frac{\partial}{\partial r} (v_0 \phi_{5n}) \end{aligned} \right\} dr + \rho_0 \phi_{1n} \left[ R' u_1 + \frac{\beta}{\rho_w c_w} p_1 (\sqrt{T+R'^2} - 1) \right]_{r=R} = 0 \quad (49)$$

### 3.4 Equations Describing the Wave Envelopes

Substitution of the assumed solution, equations (19) and (20), into equation (49) yields the following 2N equations for the A's:

$$\sum_{n=1}^{2N} f_{mn} \frac{dA_n}{dx} = \sum_{n=1}^{2N} g_{mn} A_n \quad (50)$$

where

$$\begin{aligned} f_{mn} = & \left[ \int_0^R \{ \phi_{1m} (\rho_0 \psi_n^u + u_0 \psi_n^R) + \phi_{2m} (\rho_0 u_0 \psi_n^u + \psi_n^p) + \phi_{3m} (\rho_0 u_0 \psi_n^v \right. \\ & \left. + \phi_{4m} \rho_0 u_0 \psi_n^w + \phi_{5m} (\rho_0 u_0 \psi_n^T - (\gamma-1) u_0 \psi_n^p) \} dr \right] e^{i f k_n dx} \quad (51) \\ g_{mn} = & - \left[ \int_0^R \left\{ \phi_{1m} \left[ \frac{\partial}{\partial x} (\rho_0 \psi_n^u + u_0 \psi_n^R) \right] - r v_0 \psi_n^R \frac{\partial}{\partial r} \left( \frac{\phi_{1m}}{\partial r} \right) \right. \right. \\ & + \phi_{2m} \left[ \rho_0 \frac{\partial}{\partial x} (u_0 \psi_n^u) + \psi_n^R \left( u_0 \frac{\partial u_0}{\partial x} + v_0 \frac{\partial u_0}{\partial r} \right) + \frac{\partial \psi_n^p}{\partial x} \right] \\ & - \psi_n^u \frac{\partial}{\partial r} (\rho_0 v_0 \phi_{2m}) + \phi_{3m} \left[ \rho_0 u_0 \frac{\partial \psi_n^v}{\partial x} + \rho_0 \psi_n^u \frac{\partial v_0}{\partial x} \right. \\ & \left. + \psi_n^R \left( v_0 \frac{\partial v_0}{\partial r} + u_0 \frac{\partial v_0}{\partial x} \right) \right] - v_0 \psi_n^v \frac{\partial}{\partial r} (\rho_0 \phi_{3m}) + \phi_{4m} \left[ \frac{\rho_0 v_0 \psi_n^w}{r} \right. \\ & \left. + \rho_0 u_0 \frac{\partial \psi_n^w}{\partial x} \right] - \psi_n^w \frac{\partial}{\partial r} (\rho_0 v_0 \phi_{4m}) + \phi_{5m} \left[ \rho_0 u_0 \frac{\partial \psi_n^T}{\partial x} + \rho_0 \psi_n^u \frac{\partial T_0}{\partial x} \right. \\ & \left. + \psi_n^R \left( v_0 \frac{\partial T_0}{\partial r} + u_0 \frac{\partial T_0}{\partial x} \right) - (\gamma-1) \left( u_0 \frac{\partial \psi_n^p}{\partial x} + \psi_n^u \frac{\partial p_0}{\partial x} + \psi_n^v \frac{\partial p_0}{\partial r} \right) \right] \\ & - \psi_n^T \frac{\partial}{\partial r} (\rho_0 v_0 \phi_{5m}) + (\gamma-1) \psi_n^p \frac{\partial}{\partial r} (v_0 \phi_{5m}) + \phi_{1m} i (k_n - k_m) \times \\ & (\rho_0 \psi_n^u + u_0 \psi_n^R) + \phi_{2m} i (k_n - k_m) (\psi_n^p + \rho_0 u_0 \psi_n^u) + \phi_{3m} i (k_n \\ & - k_m) \rho_0 u_0 \psi_n^v + \phi_{4m} i (k_n - k_m) \rho_0 u_0 \psi_n^w + \phi_{5m} i (k_n - k_m) u_0 \times \\ & \left. (\rho_0 \psi_n^T - (\gamma-1) \psi_n^p) \right\} dr + \rho_0 \phi_{1m} \left[ R' \psi_n^u + \frac{\beta}{\rho_w c_w} \psi_n^p (\sqrt{T + R'^2} \right. \\ & \left. - 1) \right] \Bigg] e^{i f k_n dx} \quad (52) \end{aligned}$$

For convenience the upstream modes are now denoted by  $A_n$ ,  $n = N + 1, \dots, 2N$ , i.e.,

$$A_{N+n} = \tilde{A}_n \quad n = 1, 2, 3, \dots, N$$

## 4. Numerical Solution

The procedures which implement the solution of Section 3 are described here, along with the form in which the results are presented.

### 4.1 Mean-flow Model

To evaluate the coefficients  $f_{mn}$  and  $g_{mn}$  of the set of ordinary-differential equations for the mode amplitudes  $A_n$ , one must specify all mean-flow variables,  $u_0, \rho_0, T_0, p_0, v_0$  and their first partial derivatives with respect to both  $x$  and  $r$ . The form of  $g_{mn}$  as given in Eq. (52) would also require some second derivatives; however, those terms involving second derivatives have been integrated by parts and the resulting expression for  $g$ , which requires only first derivatives of the mean flow, has been used in the numerical development. Any suitable method of solution for the mean flow can be used in conjunction with the acoustic program provided it is capable of supplying the variables and their first derivatives and provided it supplies velocity fields which satisfy the no-slip boundary condition at the wall.

For the present study, a simplified model of the mean flow has been employed. This model uses one-dimensional gas-dynamics theory to describe the mean-flow variables in the inviscid core; thus  $u_0, p_0, T_0$  and  $\rho_0$  are constant across the duct cross section except in the region of the wall boundary layer. The program permits one to select one of two options: the radial velocity  $v_0$  can be set equal to zero, consistent with the one-dimensional theory, or the radial velocity can be calculated to be a linear function of  $r$ , consistent with the mean-continuity equation and the flow tangency condition at the wall. The velocity profile in the wall boundary layer is taken to be a quarter-sine profile; that is,

$$\frac{u_0}{u_c} = \sin[\pi(R - r)/2\delta] \quad r \geq R - \delta$$

$$= 1 \quad r \leq R - \delta \quad (53)$$

The temperature profile is related to the velocity profile by<sup>56</sup>

$$\frac{T_0}{T_c} = 1 + r_1 \frac{\gamma-1}{2} M_c^2 [1 - (\frac{u_0}{u_c})^2] + \frac{T_w - T_{ad}}{T_c} [1 - \frac{u_0}{u_c}] \quad (54a)$$

$$T_{ad}/T_c = 1 + r_1 \frac{\gamma-1}{2} M_c^2 \quad (54b)$$

where the subscript c refers to values in the inviscid core,  $T_w$  is the wall temperature,  $T_{ad}$  is the adiabatic wall temperature,  $\delta$  is the boundary-layer thickness,  $r_1$  is the recovery factor, and  $\gamma = 1.4$  is the ratio of the gas specific heats. The quarter-sine profile is a good approximation for acoustic studies for cases of laminar mean flow<sup>61</sup>.

The temperature-profile formula, Eq. (54), is a good approximation for laminar boundary layers in zero pressure gradients; in this case, the recovery factor  $r_1$  is taken to be equal to  $Pr^{1/2}$  for best results, although many boundary-layer studies have been based on  $r_1 = 1$ . Since the present study is concerned with variable-area ducts, the use of Eq. (54) should be considered a rough approximation only, providing the user with a means of checking the sensitivity of the results to changes in the mean-temperature profile. To this end, three options have been provided in the program for selection of the wall temperature: the wall temperature can be set to any specified constant value, it can be set equal to the inviscid core value,  $T_c$ , or it can be set equal to the adiabatic wall temperature,  $T_{ad}$ . It is noted that if one selects the second option,  $T_w = T_c$ , and also sets  $r_1 = 0$  (no aerodynamic heating) the mean temperature will be constant across the duct width and the temperature-profile refractive effect will be eliminated; this is of value for attempting comparisons with one-dimensional results or incompressible mean-flow results.

The axial variation of the boundary-layer displacement thickness  $\delta_1$  is assumed to be known and is specified in the program by a simple polynomial variation:

$$\delta_1/\delta_{10} = [1 + b_1(x/L) + b_2(x/L)^2]R \quad (55)$$

The displacement thickness and the Mach number within the uniform core have prescribed values,  $\delta_{10}$  and  $M_{C_0}$ , at  $x = 0$ ; the subsequent axial variations of  $\delta$  and  $M_c$  are calculated within the program from the definition of displacement thickness and from mass-flow considerations. The one-dimensional gas-dynamics theory provides the axial variation of  $T_c$ ,  $\rho_c$ ,  $u_c$ , etc. and the boundary-layer profiles are computed from Eqs. (53) and (54). Thus, the mean flow within the duct is prescribed completely by input of the values of  $M_{C_0}$ ,  $\delta_{10}$ ,  $b_1$ ,  $b_2$ ,  $r_1$ ,  $\gamma$ , and  $T_w$  to the program.

## 4.2 Wall Admittance

The wall of the duct is assumed to be lined and two options are available to the user: the duct has a point-reacting liner of constant properties whose specific admittance is described by

$$\beta = \frac{1}{R_e(1-i\omega/\omega_0) + i \cot(\omega d/T_w^{1/2})} \quad (56)$$

where  $R_e$  is the resistance of a facing sheet,  $\omega_0$  is the characteristic frequency of the facing sheet, and  $d$  is the depth of the backing cavities in the liner; or the admittance of the liner can be taken to vary from a specified value  $\beta_0$  at  $x = 0$  to a specified value  $\beta_L$  at  $x = L$  according to the expression

$$\beta = \beta_0 + (\beta_L - \beta_0)(3 - 2x/L)(x/L)^2 \quad (57)$$

This latter expression gives a continuously varying admittance with  $d\beta/dx = 0$  at both  $x = 0$  and  $x = L$ .

## 4.3 Parallel-Duct Eigenfunctions

To calculate the changes in the amplitude of the acoustic wave first requires the eigenfunctions  $\psi_n$ . The number of radial modes to be considered and the mode eigenvalues at  $x = 0$  must be specified as input to the program. The quasi-parallel acoustic equations (29) and (30) are solved at each axial position by using a fourth-order Runge-Kutta forward-integration technique and by employing a Newton-Raphson procedure to determine the eigenvalues  $k_n$ . The accuracy of the Runge-Kutta procedure should assure good numerical results with a minimum of grid points across the duct width.

To determine the coefficients  $g_{mn}$  of equation (52), one has to evaluate the axial gradients of the wavenumber,  $k$ , and of the eigenfunctions  $\psi_n$ . These axial derivatives can be obtained by differentiating equations (29) and (30) with respect to the axial co-ordinate  $x$ , or by using a simple finite-difference quotient such as

$$\left. \frac{dk}{dx} \right|_x \approx \frac{k_{x+\Delta x} - k_{x-\Delta x}}{2\Delta x} \quad (58)$$

Although the first approach is more elegant and inherently more accurate it is somewhat tedious to implement for this case and would lead to longer computation times. Thus the second approach is used even though it introduces truncation errors of order  $\Delta x^2$ ; convergence checks using calculations with different values of  $\Delta x$  have shown that this is not a problem.

#### 4.4 Numerical Integration

The adjoint functions are found from the quasi-parallel-flow variables  $\psi^p$ ,  $\frac{\partial \psi^p}{\partial x}$ , and  $k$  by using the relations (39)-(43). The coefficients  $f_{mn}$  and  $g_{mn}$  are then evaluated from equations (51) and (52). The integrals across the duct in these expressions are evaluated using Simpson's rule which yields a high level of accuracy. The axial integrals  $\int k_n dx$  are evaluated with the trapezoid rule which is of sufficient accuracy to obtain good convergence with changes in  $\Delta x$ .

Writing equation (50) in matrix form,  $F dA/dx = GA$ , and solving for  $dA/dx$ , one obtains

$$\frac{dA}{dx} = F^{-1}GA \quad (59)$$

where  $A$  is a column vector whose elements are the  $A_n$ . A Runge-Kutta forward-integration technique is used to solve equations (59) for the function  $A$  at each axial station. Since the problem is linear, one can determine the solution for any problem subject to general boundary conditions at the two ends of the duct by a linear combination of  $2N$  linearly independent solutions.

The linearly independent solutions are obtained by setting all mode amplitudes except one equal to zero at  $x = 0$  and integrating equation (59) to  $x = L$ . One such integration for each of the  $2N$  modes allows one to obtain the transfer matrices  $TR_1, TR_2, TR_3, TR_4$  which are defined by

$$B^+(L) = TR_1 B^+(0) + TR_2 B^-(0) \quad (60a)$$

$$B^-(L) = TR_3 B^+(0) + TR_4 B^-(0) \quad (60b)$$

where  $B^+(x)$  is a column vector of the amplitudes  $A_n e^{i \int k_n dx}$  of the right-running modes and  $B^-(x)$  is a column vector of the amplitudes  $\tilde{A}_n e^{-i \int k_n dx}$  of the left-running modes. The transfer matrices thus allow

one to calculate the complex mode amplitudes at  $x = L$  from those at  $x = 0$ . Following reference 59, we derive results in the form of transmission and reflection coefficients for the variable-area segment being considered. The transmission and reflection coefficients relate the complex magnitudes of the outgoing modes to those of the incoming modes,

$$B^+(L) = T^{L,0}B^+(0) + R^{L,L}B^-(L) \quad (61a)$$

$$B^-(0) = T^{0,L}B^-(L) + R^{0,0}B^+(0) \quad (61b)$$

and are calculated from the transfer matrices by<sup>55</sup>

$$\begin{aligned} T^{0,L} &= TR_4^{-1} \\ R^{0,0} &= -TR_4^{-1}TR_3 \\ R^{L,L} &= TR_2TR_4^{-1} \\ T^{L,0} &= TR_1 + TR_2R^{0,0} \end{aligned} \quad (62)$$

The reflection coefficients are the negative of those defined in reference 59 as a consequence of the use of the positive sign on the  $\psi_n^p$  term in equation (19). The  $(m,n)$  term of  $T^{L,0}$  represents the transmission of the  $m^{\text{th}}$  radial mode at  $x = L$  due to the  $n^{\text{th}}$  radial mode being incident at  $x = 0$ , etc. The requirement that the procedure be able to calculate these transmission and reflection coefficients makes a direct numerical procedure undesirable for this study. The wave-envelope, eigenfunction-expansion procedure developed in Section 3 is better suited to the the necessary repetitive calculations with each mode as input than a direct numerical approach would be. Further, it is noted that the transmission and reflection coefficients are general; no assumption about the nature of the source input to the duct has been made.

#### 4.5 Acoustic Pressure Profiles

Although the procedure developed here is primarily intended to obtain transmission and reflection coefficients, the acoustic pressure distributions can be constructed if the input to the duct section is specified. Specifically, one must designate the values of  $B^+(0)$  and  $B^-(L)$  which are the amplitudes of the right-running modes that are in-

cident on the duct section at  $x = 0$  and the amplitudes of the left-running modes that are incident on the duct section at  $x = L$ , respectively. Equation (61b) then yields the value of  $B^-(0)$ . A generalization of equation (60),

$$\begin{aligned} B^+(x) &= TR_1 B^+(0) + TR_2 B^-(0) \\ B^-(x) &= TR_3 B^+(0) + TR_4 B^-(0) \end{aligned} \quad (63)$$

where the transfer matrices are functions of the axial coordinate  $x$ , is used to calculate the mode amplitudes throughout the duct. The program has been constructed to store the necessary values of the transfer matrices. Finally, the pressure distribution across the duct at each axial position is obtained from equations (10) and (19) and the definition of  $B^+$  and  $B^-$ :

$$p_1(r, x, \theta, t) = \left[ \sum_{n=1}^N B_n^+(x) \psi_n^D(r, x) + \sum_{n=1}^N B_n^-(x) \tilde{\psi}_n^D(r, x) \right] e^{i(m\theta - \omega t)} \quad (64)$$

where the bracketed terms describe the spatial distribution of interest. A similar expression is evaluated for the acoustic particle velocity (axial component) and the moduli and arguments of these quantities are output of the program.

The accuracy of these acoustic pressure and velocity profiles depends on the accuracy of the eigenfunction-expansion procedure that forms the basis of this study. General guidelines are available from parallel-duct studies, for example, Hersh and Catton<sup>62</sup> and Unruh and Eversman<sup>63</sup>; eigenvalues and attenuation rates (transmission and reflection coefficients in the variable-area case) converge more rapidly with an increasing number of basis functions than do the eigenfunctions (pressure profiles in the variable-area case). By using the parallel-duct eigenfunctions as the basis functions, we should minimize any convergence problems if all cut-on modes are included in the analysis; the magnitudes of any cut-off modes should be sufficiently small so as not to cause a large error. In addition, the integrability constraint developed in Section 3.3 assures that the governing equations are satisfied "on the average" at each cross section; that is, the average

error at any cross section will be zero even if an inadequate number of modes is used. Thus the overall characteristics of the duct such as transmission and reflection coefficients are more accurate than the details of the acoustic pressure distributions.

#### 4.6. Energy Flux

When the acoustic pressure and velocity distributions are obtained, an evaluation of an energy-flux expression is possible. We have used the expression developed by Morfey<sup>64</sup> (and others) in the computer program developed for this study; the reader is cautioned, however, that in the presence of a mean flow with strong vorticity, the "acoustic energy" as defined by this expression is not conserved. Morfey points out that there are production terms present unless the mean flow is irrotational. Alternative expressions for the energy flux are also of questionable value for the current study. The expression developed by Eversman<sup>65</sup> (and others) is restricted to uniform mean flows and the expression developed by Möhring<sup>66</sup> while permitting rotational mean flows does not allow for mean flows in which vorticity is developed as the mean flow moves in the axial direction and thus is unsuitable for the variable-area cases of interest in this study. Whether any of these expressions are of value for studies of variable-area ducts with developing mean flows that have wall shear layers is questionable. For a few simple cases with no mean flow or low-speed mean flow any of the expressions provides a check on the validity of the method of solution and its computational implementation.

## 5. Sample Cases

The computer program described in the previous section has been developed and used to provide a number of sample results. These sample results serve three purposes: to test the validity of the program and the method of analysis; to indicate the range of mean-flow and acoustic parameters for which the analysis is useful and simultaneously mark potential problems that may develop; and to provide a set of test cases that can be used by anyone who wishes to become familiar with the use of the program. To assist with this last requirement, each case contains a complete set of the input variables that were used to run the case.

All cases were run in single precision on the IBM 370 at VPI&SU; many of them have also been checked with a version of the program implemented on the CDC Cyber 175 at Langley Research Center. In most of the test cases, the duct radius is assumed to have a simple converging-diverging variation with axial distance:

$$R = 1 + a_2[-1 + \cos(2\pi x/L)] \quad (65)$$

where  $a_2$  specifies the magnitude of the variation in the outer wall and  $L$  is the length of the duct. If one wishes to consider only a converging (or diverging) duct, the program allows the calculations to be terminated at  $x = L/2$ . For other geometric variations, one must alter the geometry subroutine in the program; these alterations are simply accomplished, and one set of cases included here requires such changes.

### 5.1 Definition of Input Variables for the Program

To permit the reproduction of the results contained in subsequent sections, the Fortran variables used as program input and, when appropriate, their correspondence to the variables used in the analysis are defined here:

#### Variables that define the mean flow

<u>Fortran Variable</u>	<u>Definition</u>
XMCO	$M_{C_0}$ , Mach number at the duct entrance
GAM	$\gamma$ , Ratio of specific heats

RCF	$r_1$ , Recovery factor
DISP20	$\delta_{10}$ , Displacement thickness at $x = 0$
B2,B3	$b_1, b_2$ , Coefficients in eq. (55) describing the displacement thickness variation
CWT	Constant value of the wall temperature
NTEMP	= 1, $T_w = \text{CWT}$ = 2, $T_w = T_{ad}$ = 3, $T_w = T_c$
NRADVL	= 0 for zero radial velocity = 1 for linear variation of the mean radial velocity

Variables that define the duct properties

A2	$a_2$ , Coefficient that determines the magnitude of the variation in the duct radius
XF	L, the duct length
NCUT	= 1, Calculations for the full converging, diverging section are carried out = 2, Calculations for only the converging portion of the duct are considered
RE	$R_e$ , Liner resistance
WO	$\omega_0$ , Characteristic frequency of the liner
DIS	d, Cavity depth of the liner
BETA0	$\beta_0$ , Liner admittance at $x = 0$ ; used only if $RE = 0$
BETAL	$\beta_L$ , Liner admittance at $x = L$ ; used only if $RE = 0$

Variables that define the acoustic signal

W	$\omega$ , Circular frequency
M	m, Circumferential mode number
NM	2N, The total number of parallel-duct modes to be used in the calculations

IVK	The initial approximations for the eigenvalues of the parallel-duct modes at $x = 0$ ; an array.
ERR	The error bound for convergence of the iterations for the parallel-duct eigenvalues

#### Variables that define the numerical procedure

NSC	The number of steps across the duct in the uniform mean flow core; must be an even number
NSB	The number of steps across the duct in the mean-flow boundary layer; must be an even number
NOS	The number of axial segments into which the duct length is divided. Flow variables and acoustic profiles are printed at the end of each segment.
NSS	The number of axial steps that each segment is sub-divided into; must be either 2 or 4. $\Delta x = 1/(NOS \text{ NSS})$

#### Variables that control output

A number of variables may be printed at the end of each duct segment to serve as diagnostic tools should a problem with the program develop. Each of the following parameters is set to zero if the corresponding printout is not desired and set to unity if it is desired.

NRITR	Prints the initial iterations on the parallel-duct eigenvalues at $x = 0$
NREGN	Prints the converged values of the parallel-duct eigenvalues at the end of each segment.
NRAMP	Prints the amplitudes of each duct mode at the end of each duct segment.

## Variables for calculating the acoustic pressure profiles

NINPCS	Specifies the number of cases for which the acoustic pressure and velocity distributions are to be calculated
BPO	$B^+(0)$ ; Mode amplitudes of the right-running modes at $x = 0$ ; an array
BML	$B^-(L)$ ; Mode amplitudes of the left-running modes at $x = L$ ; an array

### 5.2 Symmetry Checks

Testing of the method of solution is somewhat difficult since there are no available solutions for acoustic propagation through variable-area ducts carrying a high-speed, compressible mean flow, except for some one-dimensional solutions. However, a few tests can be conducted for simple flows to determine internal consistency of the program.

For straight, uniform ducts, the wave-envelope amplitudes are correctly calculated to be constant throughout the duct, and the routine for solving the parallel-duct eigenfunctions and eigenvalues produces the expected results. In addition, a number of checks on the transmission and reflection coefficients have been performed for both straight and variable-area ducts with and without liners and with and without mean flows. A few of these symmetry checks are presented here.

#### (a) Straight, lined duct with no mean flow.

Since the duct is uniform, the reflection coefficients should be identically zero, and the off-diagonal terms of the transmission matrices should be zero; further,  $T^{L,0}$  should be equal to  $T^{0,L}$  because the left-running and right-running modes are identical. Results for the transmission and reflection coefficients for one such case are

$$T^{L,0} = T^{0,L} = \begin{bmatrix} -.241041 - .781958i & .000014 + .000012i \\ -.000022 - .000018i & .551753 + .671203i \end{bmatrix}$$
$$R^{0,0} = R^{L,L} = \begin{bmatrix} .000000 - .000000i & .000002 + .000001i \\ -.000003 - .000001i & .000000 + .000000i \end{bmatrix}$$

The expected results are achieved to a suitable degree of accuracy with errors in the intermodal coupling being larger than those in reflection of the modes. The input data for this case are  $W = 5$ ,  $M = 0$ ,  $NM = 4$ ,  $IVK = 5.35 + 0.1i$ ,  $3.58 + .07i$ ,  $- 5.35 - 0.1i$ ,  $-3.58 - .07i$ ,  $ERR = 10^{-4}$ ,  $XMCO = 0.0$ ,  $GAM = 1.4$ ,  $RCF = 1.0$ ,  $CWT = 1.0$ ,  $NTEMP = 1$ ,  $DISP20 = .01$ ,  $B2 = B3 = 0.0$ ,  $NRADVL = 0$ ,  $A2 = 0.0$ ,  $XF = 2.0$ ,  $NCUT = 1$ ,  $RE = 0.8$ ,  $WO = 15$ ,  $DIS = .05$ ,  $NSC = 16$ ,  $NSB = 2$ ,  $NOS = 20$ ,  $NSS = 2$ ,  $NINPCS = 0$ . Note that one must specify a non-zero boundary-layer thickness which, for cases of no mean flow, is strictly an expedient for setting up the numerical steps across the duct. In this case the number of steps in the "boundary layer" is set to the minimum possible value since the "boundary-layer thickness" is small.

(b) Variable-area lined duct with no mean flow.

In this case, reflection and intermodal coupling in the transmission coefficients is expected to be non-zero; however, the symmetry of the situation still requires  $T^{0,L} = T^{L,0}$  and  $R^{0,0} = R^{L,L}$ . For one such case, the results are

$$T^{L,0} = \begin{bmatrix} -.17802 - .63795i & -.33815 - .16619i \\ -.50851 - .24930i & .57103 - .24494i \end{bmatrix}$$

$$T^{0,L} = \begin{bmatrix} -.17803 - .63804i & -.33818 - .16623i \\ -.50856 - .24936i & .57110 - .24497i \end{bmatrix}$$

Errors are typically in the fifth decimal place with the maximum error in the fourth decimal place. The reflection coefficients agree to five decimal places, and

$$R^{0,0} = \begin{bmatrix} .00426 + .01666i & -.03609 + .04866i \\ .05460 + .07300i & -.14420 - .14625i \end{bmatrix}$$

The input data for this case are the same as those in part (a) except that  $A2 = 0.1$ .

(c) Variable-area lined duct with mean flow

In this case the transmission coefficients  $T^{L,0}$  for a case when  $M > 0$  (mean flow from left to right) should be the same as the coefficients  $T^{0,L}$  for a case when  $M < 0$  (mean flow from right to left) provided all duct properties and the mean flow are symmetric about  $x = L/2$ . Similar arguments can be made for the reflection coefficients. An example of such results yields

for  $M_{c_0} = -0.3$ ,

$$T^{L,0} = \begin{bmatrix} .51771 + .29426i & .37739 - .27368i \\ .38645 - .31743i & -.06760 + .36536i \end{bmatrix}$$

and for  $M_{c_0} = +0.3$

$$T^{0,L} = \begin{bmatrix} .51790 + .29418i & .37744 - .27382i \\ .38650 - .31753i & -.06748 + .36548i \end{bmatrix}$$

The agreement between  $T^{0,L}$  for  $M_0 = -0.3$  and  $T^{L,0}$  for  $M_0 = +0.3$ , is comparable to that shown above and the agreement for reflection coefficients is better. The results are relatively insensitive to changes in the error bound on the eigenvalues of the parallel duct; changes in the numerical step sizes will alter the values of the transmission coefficients but do not change the general conclusions concerning the self consistency of the results. Since the largest errors are in the fourth decimal place, the results are considered to be satisfactory.

The input data for the above results for  $T^{L,0}$  are  $W = 10$ ,  $M = 0$ ,  $NM = 4$ ,  $IVK = 7.2 + .08i$ ,  $5.3 + .22i$ ,  $-13.9 - .04i$ ,  $-12.3 - .20i$ ,  $ERR = 10^{-4}$ ,  $XMCO = 0.3$ ,  $GAM = 1.4$ ,  $RCF = 1.0$ ,  $CWT = 1.0$ ,  $NTEMP = 1$ ,  $DISP20 = .01$ ,  $B2 = B3 = 0.0$ ,  $NRADV L = 0$ ,  $A2 = 0.12$ ,  $XF = 2.0$ ,  $NCUT = 1$ ,  $RE = 0.8$ ,  $WO = 15$ ,  $DIS = .05$ ,  $NSC = 16$ ,  $NSB = 8$ ,  $NOS = 20$ ,  $NSS = 2$ ,  $NINPCS = 0$ . For calculating  $T^{0,L}$  the input data was the same except for  $XMCO = -0.3$ , and  $IVK = 13.9 + .04i$ ,  $12.3 + .20i$ ,  $-7.2 - .08i$ ,  $-5.3 - .22i$ . The mean flow Mach number in these cases reaches a value of .61 at the throat of the duct, sufficiently large that compressibility effects in the mean flow are important.

### 5.3 Comparison with one-dimensional theory

For a one-dimensional mean flow and acoustic disturbance, results are available in the literature; for example, Myers and Callegari<sup>1</sup> use such calculations to indicate the singular behavior of linear acoustic theory as the mean Mach number approaches unity. For their calculations, the duct area is described by a polynomial

$$R^2 = \frac{1}{2} \left[ 1 + 8\left(\frac{X}{L} - \frac{1}{2}\right)^2 - 16\left(\frac{X}{L} - \frac{1}{2}\right)^4 \right]$$

and results are presented in the form of the ratio of the acoustic pressure amplitude to the incident pressure amplitude as a function of distance through the duct.

The wave-envelope method clearly is not a one-dimensional model; however, as many two-dimensional effects as possible have been suppressed to effect the closest possible agreement between conditions in the one-dimensional calculations and the wave-envelope calculations. Only one mode propagating in each direction is included, and the duct wall is taken to be rigid. The boundary-layer displacement thickness is set to a very small value (.001) in an attempt to minimize any refractive effects on the acoustic signal. In order to obtain the same axial variation of the mean flow in both calculations, the radius of the duct for the wave-envelope calculations has been taken to be

$$R = \left\{ \frac{1}{2} \left[ 1 + 8\left(\frac{X}{L} - \frac{1}{2}\right)^2 - 16\left(\frac{X}{L} - \frac{1}{2}\right)^4 \right] \right\}^{1/2} + \delta_1$$

and the displacement thickness is taken to be constant

$$\delta_1 = \delta_{10} = .001$$

These expressions require that the geometry subroutine of the program be altered if one wishes to reproduce the results of this section. To suppress two-dimensional effects, the mean radial velocity has been set to zero; the wall temperature is taken to be equal to the value at the centerline and the recovery factor has been set to zero in order to eliminate any refractive effect from a transverse temperature gradient. Despite these restrictions, the wave-envelope method is still basically two dimensional: for example, the acoustic particle velocity normal to the wall is required to be zero whereas a one-dimensional model is equivalent to a zero acoustic velocity normal to the duct centerline.

Hence it is of interest to examine the differences between the results of the two approaches. In general, it has been found that the magnitude of the acoustic pressure is larger near the throat of the duct than is predicted by one-dimensional theory, especially when the throat Mach number is large. In addition, as the throat Mach number reaches high subsonic values, a substantial refractive effect develops, even from the very small boundary layer that was used in this study. An example of these effects is shown in Fig. 2. The converging duct section results in a higher acoustic pressure in the throat region than is predicted by one-dimensional theory. The incident signal at  $x = 0$  propagates downstream, and an upstream wave is present as a consequence of reflection within the variable-area duct. In the throat region the upstream wave has a very short wavelength and thus the boundary layer produces a significant refraction of the upstream wave toward the duct centerline. The acoustic propagation in the throat region is not a one-dimensional process.

The effect of removing some of the "one-dimensional" restrictions has been examined. The results of Fig. 3 have been obtained with a constant wall temperature throughout the duct,  $T_w = 1.0$ ; thus the wall is hotter than the mean flow in the vicinity of the throat and a temperature-profile refractive effect occurs. This results in a further intensification of the acoustic pressure in the throat region. Finally the influence of a mean radial velocity has been included, and the results are shown in Fig. 4. The mean radial velocity component has a strong effect on the acoustic pressure, reducing the pressure amplitude at the throat and bringing the two-dimensional results into closer agreement with one-dimensional theory than occurred in the two previous cases. Input data for reproducing the case in Fig. 2 are  $W = 1.009$ ,  $M = 0$ ,  $NM = 2$ ,  $IVK = 7.77 + 0.0i$ ,  $-14.38 + 0.0i$ ,  $ERR = 10^{-3}$ ,  $XMCO = .299$ ,  $GAM = 1.4$ ,  $RCF = 0.0$ ,  $NTEMP = 3$ ,  $DISP20 = .001$ ,  $NRADVL = 0$ ,  $XF = 1.0$ ,  $NCUT = 1$ ,  $RE = 0.0$ ,  $BETA0 = 0.0 + 0.0i$ ,  $BETAL = 0.0 + 0.0i$ ,  $NSC = 14$ ,  $NSB = 10$ ,  $NOS = 40$ ,  $NSS = 2$ ,  $NINPCS = 1$ ,  $BPO = 1/\sqrt{2}$ ,  $0.0$ , etc.,  $BML = 0.0$ . For Fig. 3, the data are the same except that  $NTEMP = 1$  and  $CWT = 1.0$ . Finally the results in Fig. 4 have the same input data as those for Fig. 3 except that  $NRADVL = 1$ .

## 5.4 Comparison with Finite-Element Results

A number of test cases have been set up for comparing the results of the wave-envelope procedure with the results from the finite-element procedure developed by Abrahamson<sup>54</sup>. The finite-element results have been supplied by H. Lester of Langley Research Center. Currently, comparisons have been made for two of the cases, and additional ones are being carried out.

The finite-element method was developed for a compressible mean flow, but is currently implemented with an incompressible model; hence the cases chosen for comparison are for low-speed mean flows or for no mean flow. The mean flow varies from  $M = -0.1$  at  $x = 0$  to  $M = -.158$  at the throat, and the mean boundary-layer thickness is assumed to be 10% of the local duct radius; the wave-envelope solution is based on a uniform mean temperature distribution across the duct. The wave-envelope method specifies the mode amplitudes incident on the duct section at  $x = 0$ , specifies no input at  $x = L$  and solves for the acoustic pressure distribution throughout the duct. The pressure distribution that results at  $x = 0$  is used as input for the finite-element program, which specifies a  $\rho_0 c_0$  impedance at  $x = L$  to approximate the no-input boundary condition at that station. The pressure profiles from the two methods at  $x/L = 1/4, 1/2, 3/4$  and  $1$ , as well as the axial variation of the pressure at the wall, are then compared.

The two cases currently available correspond to an input signal of 500 Hz in a 2-meter-diameter rigid duct with the mean speed of sound being 344.4m/sec. These conditions yield a dimensionless circular frequency of  $\omega = 9.12$  at which there are three cut-on modes propagating in each direction. The comparison for no mean flow is shown in Fig. 5. The incident signal at  $x = 0$  is the fundamental, plane mode and reflection in the duct results in the acoustic distribution shown in the left portion of the figure. Considerable variation of the acoustic profiles takes place as the signal propagates through the duct. The trends from the two methods of solution are the same, and the results agree reasonably well except at the center of the duct near the throat. The variation of pressure along the outer wall is also quite pronounced, and both methods

yield the same trends: the peak magnitude occurs ahead of the minimum area and a local minimum in pressure occurs close to the minimum area. Although the agreement is not exact, overall it is very satisfactory.

The transmission coefficient  $T^{L,0}$  and reflection coefficient  $R^{0,0}$  for this case are

$$T^{L,0} = \begin{bmatrix} .823-.519i & .106-.040i & .085-.114i \\ .118-.045i & -.703-.532i & .085+.361i \\ .135-.181i & .121+.514i & -.342+.727i \end{bmatrix}$$

and

$$R^{0,0} = \begin{bmatrix} .003-.012i & .010+.018i & -.049+.014i \\ .011+.020i & -.027-.015i & .058-.067i \\ -.077+.021i & .082-.094i & .276+.180i \end{bmatrix}$$

The intermodal coupling coefficients (the off-diagonal terms of  $T^{L,0}$ ) are an order of magnitude larger than the reflection coefficients, and it is this coupling between modes that is primarily responsible for the variations of the acoustic profiles throughout the duct. Despite the small values of the reflection coefficients, they have a noticeable effect on the acoustic pressure distribution as seen in Fig. 5 by comparing the incident signal with the total signal at  $x = 0$ . The input data to reproduce this result are  $W = 9.12$ ,  $M = 0$ ,  $NM = 6$ ,  $IVK = 9.12$ ,  $8.28$ ,  $5.83$ ,  $-9.12$ ,  $-8.28$ ,  $-5.83$ ,  $ERR = 10^{-3}$ ,  $XMCO = 0.0$ ,  $GAM = 1.4$ ,  $RCF = 0.0$ ,  $NTEMP = 3$ ,  $DISP20 = .0363$ ,  $B2 = B3 = 0.0$ ,  $NRADVL = 0$ ,  $A2 = 0.1$ ,  $XF = 2.0$ ,  $NCUT = 1$ ,  $RE = 0.0$ ,  $BETA0 = BETAL = 0.0$ ,  $NSC = 20$ ,  $NSB = 2$ ,  $NOS = 16$ ,  $NSS = 2$ ,  $NINPCS = 1$ ,  $BPO = 1/\sqrt{2}$ ,  $0.0$ , etc.

A similar comparison has been made when the input signal propagates upstream against the mean flow. The results are shown in Fig. 6 and are very similar to those for no mean flow. The mean boundary layer causes a refraction of the disturbance away from the duct wall as expected; the differences between the finite-element and wave-envelope results are very large in the throat region near the duct centerline but otherwise are comparable to those found in the case without flow. Both methods "conserve energy" to a suitable level of accuracy. The transmission matrix  $T^{L,0}$  is

$$\Gamma^{L,0} = \begin{bmatrix} -.314+.909i & -.045+.113i & -.003+.190i \\ -.050+.124i & .816+.087i & -.329-.335i \\ -.005+.286i & -.449-.457i & -.050-.763i \end{bmatrix}$$

Again the intermodal coupling in transmission is quite strong. Input data for reproduction of the results are the same as those for the no-mean-flow case, except for  $XMCO = -0.1$ ,  $NRADVL = 1$ ,  $NSB = 8$ , and  $IVK = 10.13, 9.29, 6.85, -8.29, -7.45, -5.01$ .

At a frequency of 1000 Hz or  $\omega = 18.24$ , there are six cut-on modes at the entrance, but the sixth mode cuts off within the duct. This situation presents difficulties for the wave-envelope calculations since it breaks down at a hard-wall cut-off point; it is also noted that if the sixth mode is not well cut on the  $\rho_0 c_0$  impedance used as a boundary condition at  $x = L$  in the finite-element program may not be adequate. The breakdown of the wave-envelope method at hard-wall cut off is the major restriction on the use of the wave-envelope procedure. The results can be obtained with only five modes, but one would expect this to introduce errors. Thus, the wave-envelope procedure is better suited for lined ducts than it is for rigid ducts.

### 5.5 Straight Ducts with Variable Liners

Several cases have been considered for wave propagation through a straight duct in which the wall admittance varies from zero at  $x = 0$  to  $\beta_L = 0.6 + 0.6i$  at  $x = L$ . Other conditions are basically the same as those discussed in Section 5.4, and ultimately a comparison of these results with the finite-element results will be made. Two results are given here, for  $\omega = 9.12$  and  $\omega = 18.24$ , both for an incident signal at  $x = 0$  that consists of two modes propagating upstream. In these cases, the reflection coefficients are so small that they do not affect the acoustic profiles. The results for the lower frequency are shown in Fig. 7 and those for the higher frequency in Fig. 8. The refraction of the signal away from the wall due to the upstream propagation is more pronounced in the high-frequency case. The acoustic amplitude along the

wall is reduced significantly as the wave propagates through the duct, but the reduction in energy flux is small in both cases (1.46dB and .34dB). The main effect of the variable liner properties is to couple the modes in transmission as shown by the transmission matrix for  $\omega = 9.12$ :

$$T^{L,0} = \begin{bmatrix} .448+.782i & .333+.052i & .007+.024i \\ -.185+.132i & .307-.632i & -.158+.062i \\ -.001+.020i & -.008-.058i & .434-.100i \end{bmatrix}$$

The first two modes interact strongly, whereas only small amounts of the third mode are generated by the presence of the first two. Input data for the low frequency case are  $W = 9.12$ ,  $M = 0$ ,  $NM = 6$ ,  $IVK = 10.13$ ,  $9.29$ ,  $6.85$ ,  $-8.29$ ,  $-7.45$ ,  $-5.01$ ,  $ERR = 10^{-3}$ ,  $XMCO = -0.1$ ,  $GAM = 1.4$ ,  $RCF = 0.0$ ,  $NTEMP = 3$ ,  $DISP20 = .0363$ ,  $B2 = B3 = 0.0$ ,  $NRADVL = 1$ ,  $A2 = 0.0$ ,  $XF = 2.0$ ,  $NCUT = 1$ ,  $RE = 0.0$ ,  $BETAO = 0.0$ ,  $BETAL = 0.6 + 0.6i$ ,  $NSC = 20$ ,  $NSB = 8$ ,  $NOS = 16$ ,  $NSS = 2$ ,  $NINPCS = 1$ ,  $BPO = 1/\sqrt{2}$ ,  $0.1-0.2i$ ,  $0$ , etc.,  $BML = 0.0$ . The higher frequency corresponds to  $W = 18.24$ ,  $IVK = 20.27$ ,  $19.86$ ,  $18.86$ ,  $17.17$ ,  $14.5$ ,  $9.93$ ,  $-16.58$ ,  $-16.17$ ,  $-15.18$ ,  $-13.48$ ,  $-10.81$ ,  $-6.25$ , with all other data the same as in the low frequency case.

## 5.6 General, Axisymmetric Case

A case is examined in which the incident signal propagates downstream in a converging-diverging duct in which the mean flow reaches a Mach number of .465 at the throat and the boundary-layer thickness grows rapidly downstream of the throat. In addition, the duct is lined with a variable-admittance liner, changing from  $\beta_0 = .5-.2i$  to  $\beta_L = .2-.1i$ . It is assumed that the mean flow has reached adiabatic conditions with the duct walls:  $T_w = T_{ad}$ . The basic physical properties are defined by a 1000 Hz signal propagating in a duct whose diameter varies over a 60.96 cm (2') axial distance from 30.48 cm (1') at the entrance to 25.4 cm (10") at the throat. Using  $c_0 = 335.28$  m/sec. (1100 ft/sec), one obtains  $\omega = 2.86$ , a frequency at which only one cut-on mode propagates in each direction. The transmission and reflection coefficients for this case are

$$\begin{aligned}
T^{L,0} &= .0683-.1636i \\
T^{0,L} &= -.0007+.0002i \\
R^{0,0} &= -.0023-.0022i \\
R^{L,L} &= -.0004+.0001i
\end{aligned}$$

Substantial reduction of the acoustic signal occurs in this case as shown by the small magnitudes of the transmission coefficients. An upstream-propagating signal would be almost eliminated. For the first right-running mode incident at  $x = 0$ , the pressure profile at  $x = L$  also is quite small compared to that at  $x = 0$ , as shown in Fig. 9; the energy flux is reduced by approximately 15.3dB. Input data for this case are  $W = 2.86$ ,  $M = 0$ ,  $NM = 2$ ,  $IVK = 2.7+.48i$ ,  $-3.16-.76i$ ,  $ERR = 10^{-3}$ ,  $XMCO = 0.3$ ,  $NRADVL = 1$ ,  $GAM = 1.4$ ,  $RCF = 0.8$ ,  $NTEMP = 2$ ,  $DISP20 = .02$ ,  $B2 = -2$ ,  $B3 = 4$ ,  $A2 = .08333$ ,  $XF = 8.0$ ,  $NCUT = 1$ ,  $RE = 0.0$ ,  $BETA0 = 0.5-0.2i$ ,  $BETAL = 0.2-0.1i$ ,  $NSC = 16$ ,  $NSB = 8$ ,  $NOS = 25$ ,  $NSS = 4$ ,  $NINPCS = 1$ ,  $BPO = 1/\sqrt{2}$ ,  $0.0$ , etc.,  $BML = 0.0$ .

### 5.7 Spinning-Mode Case

All the previous sample calculations considered axisymmetric acoustic waves. The program also can be used to study cases involving spinning modes as illustrated by a case for  $m = 2$ . The input signal of frequency  $\omega = 7$  propagates downstream in a variable-area duct with constant liner properties. The acoustic pressure profiles at several axial positions along with the wall pressure variation are shown in Fig. 10; these profiles correspond to the lowest radial mode being incident at  $x = 0$  and are calculated with the two cut-on radial modes propagating in each direction. Transmission and reflection coefficients in this calculation are

$$\begin{aligned}
T^{L,0} &= \begin{bmatrix} .475+.097i & -.030-.066i \\ -.078-.144i & .013+.062i \end{bmatrix} \\
R^{0,0} &= \begin{bmatrix} .008-.026i & .108+.011i \\ .257+.031i & .336+.567i \end{bmatrix}
\end{aligned}$$

It is seen that the second downstream mode is strongly reflected into two upstream-propagating modes with relatively little of the mode

passing through the duct section. This effect is not seen in Fig. 10 since it corresponds to the case when only the lowest mode is incident on the duct section. Input data for these calculations are  $W = 7.0$ ,  $M = 2$ ,  $NM = 4$ ,  $IVK = 6.4+.32i$ ,  $2.47+.25i$ ,  $-8.4-.63i$ ,  $-4.04-.28i$ ,  $ERR = 10^{-3}$ ,  $XMCO = 0.1$ ,  $GAM = 1.4$ ,  $RCF = 0.0$ ,  $NTEMP = 3$ ,  $DISP20 = .0363$ ,  $B2 = 0.5$ ,  $B3 = 0.5$ ,  $NRADVL = 1$ ,  $A2 = 0.1$ ,  $XF = 2.0$ ,  $NCUT = 1$ ,  $RE = 0.8$ ,  $WO = 15.0$ ,  $DIS = .05$ ,  $NSC = 20$ ,  $NSB = 8$ ,  $NOS = 16$ ,  $NSS = 2$ ,  $NINPCS = 1$ ,  $BPO = 1/\sqrt{2}$ ,  $0.0$ , etc.,  $BML = 0.0$ .

The numerical solution for the parallel-duct eigenfunctions and eigenvalues can be expected to become increasingly inaccurate as the spinning mode number increases. For  $m \geq 5$  some caution should be used and for  $m \geq 10$  numerical difficulties and inaccuracies are to be expected. These high spinning modes will require an asymptotic expansion technique for accurate computation.

### 5.8 Convergence of Results with Number of Modes

It has been previously stated that one expects the results to be accurate if all cut-on modes are included in the calculation. In this section, a case for  $\omega = 18$  is considered in which there are six cut-on modes in each direction. Calculations are made with fewer modes in order to check the convergence of the results as the number of modes is increased. The case discussed here is a straight duct with no mean flow and lined with a variable-admittance liner. Figure 11 shows the various approximations to the pressure profile at  $x = L/2$  for the case when the lowest mode is input at  $x = 0$ . It is seen that convergence is slowest at the duct centerline, fastest at the wall, and that changes are quite pronounced across the entire duct for the first four modes. Addition of the fifth and sixth modes produces small changes (this would not be true if the input signal contained significant amounts of these modes). In contrast, the transmission coefficients converge more rapidly as shown in Table 1. With four modes, the transmission coefficients of all the modes that can be calculated are accurate. The coefficient of the lowest mode is the slowest to converge. Input data for calculations of these cases are  $W = 18.0$ ,  $M = 0$ ,  $IVK = 18.0$ ,  $17.59$ ,  $16.58$ ,  $14.85$ ,  $12.11$ ,

7.26, -18.0, -17.59, -16.58, -14.85, -12.11, -7.26,  $ERR = 10^{-3}$ ,  $XMCO = 0.0$ ,  $GAM = 1.4$ ,  $RCF = 0.0$ ,  $NTEMP = 3$ ,  $DISP20 = .0363$ ,  $B2 = B3 = 0.0$ ,  $NRADV L = 0$ ,  $A2 = 0.0$ ,  $XF = 2.0$ ,  $NCUT = 1$ ,  $RE = 0.0$ ,  $BETA0 = 0.0$ ,  $BETAL = 0.6 + 0.6i$ ,  $NSC = 20$ ,  $NSB = 2$ ,  $NOS = 16$ ,  $NSS = 2$ ,  $NINPCS = 1$ ,  $BPO = 1/\sqrt{2}$ ,  $0.0$ , etc.,  $BML = 0.0$ . The value of  $NM$  changes from 2 to 12 as the number of modes is changed.

TABLE 1. Effect of increasing the number of modes on the convergence of the transmission coefficients.

N	$T_{11}^{L,0}$	$T_{12}^{L,0}$	$T_{13}^{L,0}$
1	-.323-.907i		
2	-.251-.828i	-.291-.349i	
3	-.238-.825i	-.309-.350i	.080+.017i
4	-.236-.826i	-.311-.348i	.081+.012i
5	-.236-.827i	-.311-.348i	.081+.012i
6	-.236-.827i	-.311-.348i	.081+.012i

	$T_{14}^{L,0}$	$T_{15}^{L,0}$	$T_{16}^{L,0}$
1			
2			
3			
4	-.012+.011i		
5	-.011+.011i	.001-.003i	
6	-.011+.011i	.001-.003i	.0005+.0001i

## 6. Summary

An acoustic theory is developed to determine the sound transmission and attenuation through an infinite, hard-walled or lined circular duct carrying compressible, sheared, mean flows and having a variable cross section. The theory is applicable to large as well as small axial variations, as long as the mean flow does not separate. The technique is based on solving for the envelopes of the quasi-parallel acoustic modes that exist in the duct instead of solving for the actual wave, thereby reducing the computation time and the round-off error encountered in purely numerical techniques. The solution recovers the solution based on the method of multiple scales for slowly varying duct geometry.

A computer program has been developed based on the wave-envelope analysis for general mean flows. The mean-flow model consists of a one-dimensional flow in an inviscid core and a quarter-sine profile in the boundary layer. Mean radial velocity effects can be included. Numerical calculations performed for waves propagating in uniform ducts carrying fully-developed mean flows agree with the well-known results for uniform ducts. For non-uniform ducts, results are presented for the reflection and transmission coefficients as well as the acoustic pressure distributions for a number of conditions: both straight and variable area ducts with and without liners and mean flows from very low to high subsonic speeds are considered. The results for transmission and reflection coefficients are shown to possess symmetry characteristics in those cases for which it is expected. Comparisons with the results of a finite-element analysis for low-speed mean flows have shown reasonable agreement. Comparisons with one-dimensional results for high-speed mean flows have shown strong two-dimensional effects occurring near the duct throat. A number of test cases that demonstrate the flexibility of the program are included. Convergence of the transmission coefficients and of the acoustic pressure profiles with an increasing number of modes is illustrated.

The only limitation of the wave envelope technique is that it is not suitable near cut-off, since the coefficient multiplying the term  $dA_n/dx$  approaches zero. This problem is more apparent for a hard wall duct than for a soft wall duct, because  $k$  is exactly zero for a hard

wall duct. Near cut off, the problem requires a turning-point analysis using either the method of multiple scales or the Langer transformation<sup>32</sup>. In addition, in a duct with very large axial gradients, such as occur in the throat region as  $M \rightarrow 1$ , small axial steps may be required to assure that the program obtains an independent set of parallel-duct eigenfunctions to serve as basis functions. If two of the eigenvalues are the same an ill-conditioned matrix results and the program terminates.

APPENDIX A  
Symbols and Notation

Symbol

$a_2$	Coefficient that specifies the minimum duct radius in Eq. (65)
$A$	Vector of mode amplitudes; $2N$ components
$A_n$	Amplitude of the $n^{\text{th}}$ right-running mode
$\tilde{A}_n$	Amplitude of the $n^{\text{th}}$ left-running mode
$b_1, b_2$	Coefficients in the expression for the axial variation of the mean boundary-layer displacement thickness, Eq. (55)
$B^+$	Vector of local amplitudes of the right-running modes; $N$ components; $n^{\text{th}}$ component = $A_n \exp\{i/k_n dx\}$
$B^-$	Vector of local amplitudes of the left-running modes; $N$ components; $n^{\text{th}}$ component = $\tilde{A}_n \exp\{i/\tilde{k}_n dx\}$
$c$	Speed of sound, $c^*/c_a^*$
$C_p$	Specific heat at constant pressure
$d$	Cavity depth of liner
$f_{mn}$	An element of one of the coefficient matrices in the governing equation for the mode amplitudes, Eq. (50)
$F$	Coefficient matrix whose components are $f_{mn}$
$g_{mn}$	An element of one of the coefficient matrices in the governing equation for the mode amplitudes, Eq. (50)
$G$	Coefficient matrix whose components are $g_{mn}$
$i$	$\sqrt{-1}$
$k_n, \tilde{k}_n$	Complex propagation coefficients of the $n^{\text{th}}$ right-running and left-running parallel-duct modes, respectively.
$L$	Duct length, $L^*/R\ddagger$
$m$	Circumferential mode number
$M$	Mach number of mean flow
$M_0$	Mach number of mean flow at $x = 0$
$N$	Number of parallel-duct modes propagating in each direction.
$p$	Pressure, $p^*/\rho_a^* c_a^{*2}$
$Pr$	Prandtl number, $\mu_w^* C_p^*/\kappa_w^*$

$q$	An arbitrary physical variable
$\vec{r}$	Position vector, $\vec{r}^*/R\ddagger$
$r$	Radial co-ordinate, $r^*/R\ddagger$
$r_1$	Recovery factor used in Eq. (54)
$R$	Duct radius, $R^*/R\ddagger$
$R_e$	Resistance of the liner facing sheet
$Re$	Reynolds number, $\rho_a^* c_a^* R\ddagger / \mu_w^*$
$R_0$	Duct radius at $x = 0$
$R^{0,0}$	Reflection coefficient matrix at $x = 0$ for modes incident at $x = 0$ ; defined by Eq. (61)
$R^{L,L}$	Reflection coefficient matrix at $x = L$ for modes incident at $x = L$ ; defined by Eq. (61)
$t$	Time, $t^* c_a^* / R\ddagger$
$T$	Temperature, $T^*/T_a^*$
$T^{L,0}$	Transmission coefficient matrix at $x = L$ for modes incident at $x = 0$ ; defined by Eq. (61)
$T^{0,L}$	Transmission coefficient matrix at $x = 0$ for modes incident at $x = L$ ; defined by Eq. (61)
$T_{ad}$	Adiabatic wall temperature; defined by Eq. (54b)
$TR_1, TR_2, TR_3, TR_4$	Transfer matrices defined by Eq. (60)
$u$	Axial velocity component, $u^*/c_a^*$
$v$	Radial velocity component, $v^*/c_a^*$
$\vec{v}$	Velocity vector, $\vec{v}^*/c_a^*$
$w$	Circumferential velocity component, $w^*/c_a^*$
$x$	Axial co-ordinate, $x^*/R\ddagger$
$\alpha$	Attenuation rate of the parallel-duct modes; imaginary part of $k$
$\beta$	Liner admittance
$\gamma$	Ratio of specific heats
$\delta$	Mean boundary-layer thickness, $\delta^*/R\ddagger$
$\delta_1$	Mean boundary-layer displacement thickness, $\delta_1^*/R\ddagger$
$\delta_{10}$	Mean boundary-layer displacement thickness at $x = 0$
$\eta$	Variable defined in the adjoint homogeneous problem, Eqs. (44) - (47)

$\theta$	Circumferential co-ordinate
$\kappa$	Thermal conductivity, $\kappa^*/\kappa_w^*$
$\mu$	Viscosity coefficient, $\mu^*/\mu_w^*$
$\rho$	density, $\rho^*/\rho_a^*$
$\underline{\underline{\tau}}$	Viscous stress tensor, $\underline{\underline{\tau}}^*/\rho_a^*c_a^{*2}$
$\phi_1, \phi_2, \phi_3, \phi_4, \phi_5, \phi_6$	Weighting functions for the mass, axial momentum, radial momentum, circumferential momentum, energy, and state equations, respectively; related to the parallel-duct eigenfunctions through Eq. (48) and Eqs. (39)-(43)
$\Phi$	Viscous dissipation function, $\Phi^*/\rho_a^*c_a^{*3}$
$\psi$	Parallel-duct eigenfunctions
$\psi^P, \psi^T, \text{etc}$	Parallel duct eigenfunctions for the acoustic pressure, temperature, etc.
$\omega$	Circular frequency, $\omega^*R\ddagger/c_a^* = 2\pi f^*R\ddagger/c_a^*$ where $f^*$ is the frequency in Hz.
$\hat{\omega}$	$\omega - ku_0$ ; Eq. (28)

### Subscripts

a	Denotes a reference quantity; taken to be a mean-flow quantity at $x = 0$ and $r = 0$ .
o	Denotes a mean-flow quantity
1	Denotes an acoustic quantity
c	Denotes a mean-flow quantity evaluated at the duct centerline
mn	Denotes a component of a matrix
n	Denotes either a quantity associated with a specific duct mode or an arbitrary component of a vector
w	Denotes a mean-flow quantity evaluated at the duct wall

### Superscripts

$( )^+$	Denotes a quantity associated with a right-running parallel-duct mode.
$( )^-$ or $( \tilde{ } )$	Denotes a quantity associated with a left-running mode
$( )^T$	Denotes the transpose of a tensor
$( )^*$	Denotes a dimensional quantity

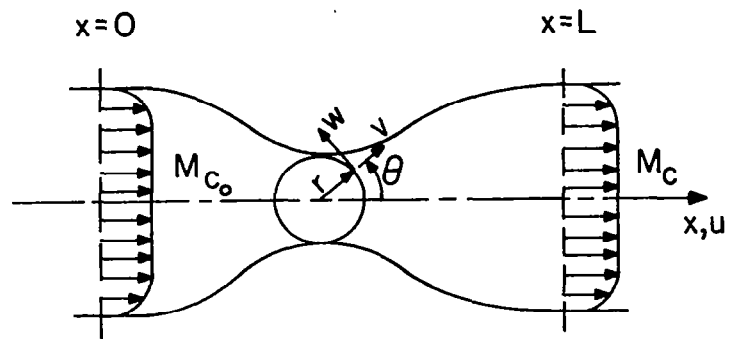


Figure 1. Flow Configuration.

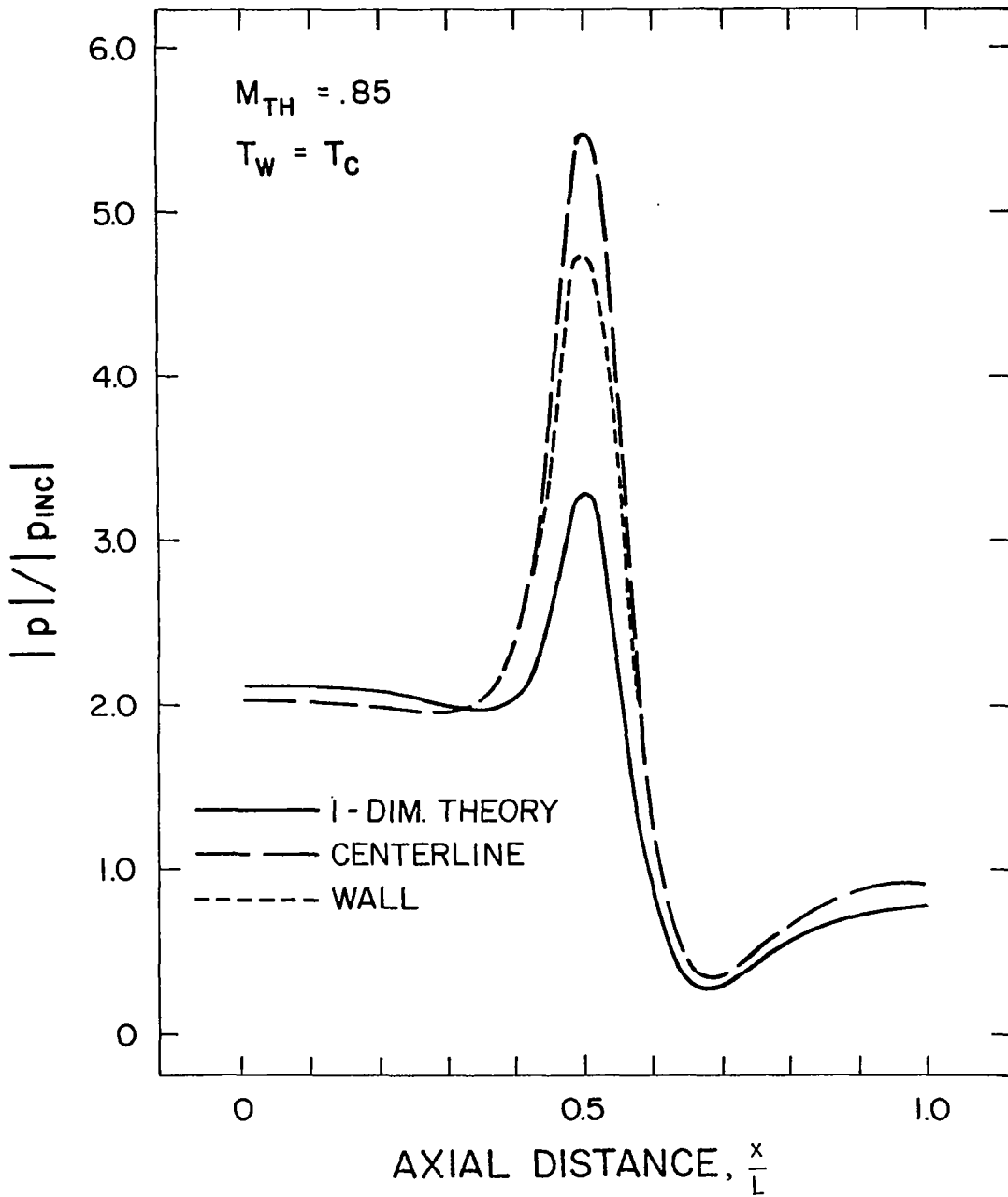


Figure 2. Comparison of wave-envelope and one-dimensional theories.

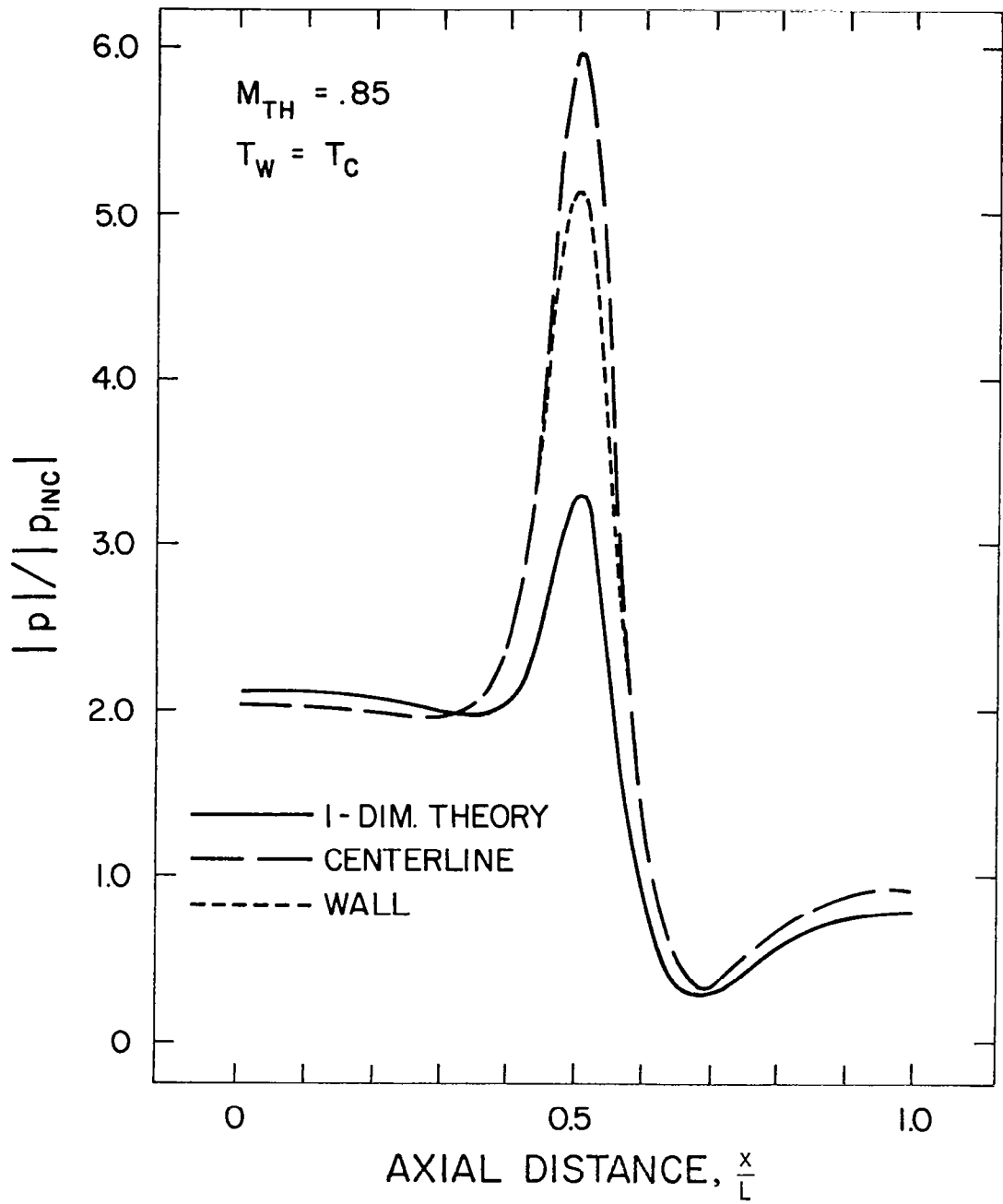


Figure 3. Comparison of wave-envelope and one-dimensional theories.

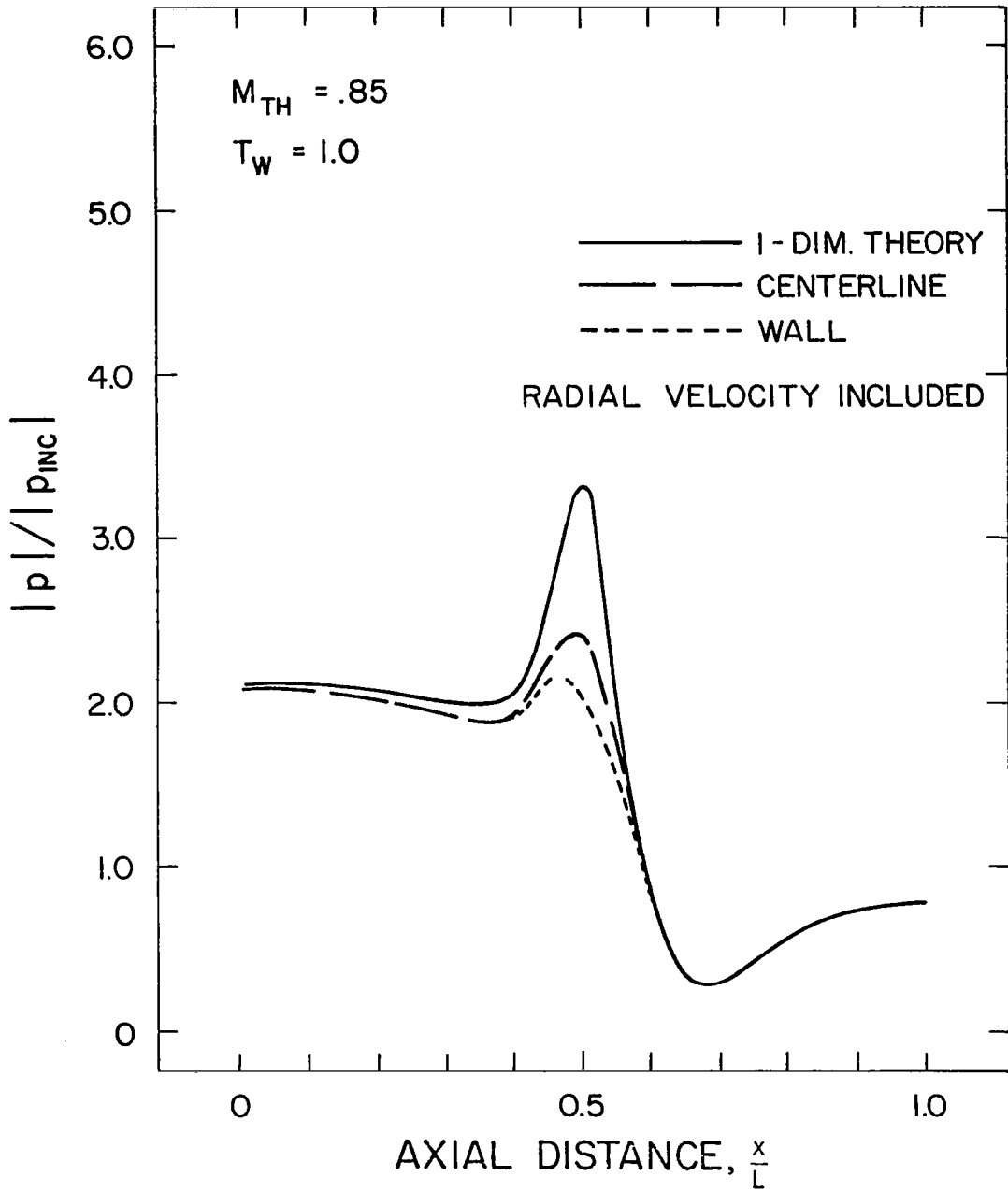


Figure 4. Comparison of wave-envelope (including radial velocity) and one-dimensional theories.

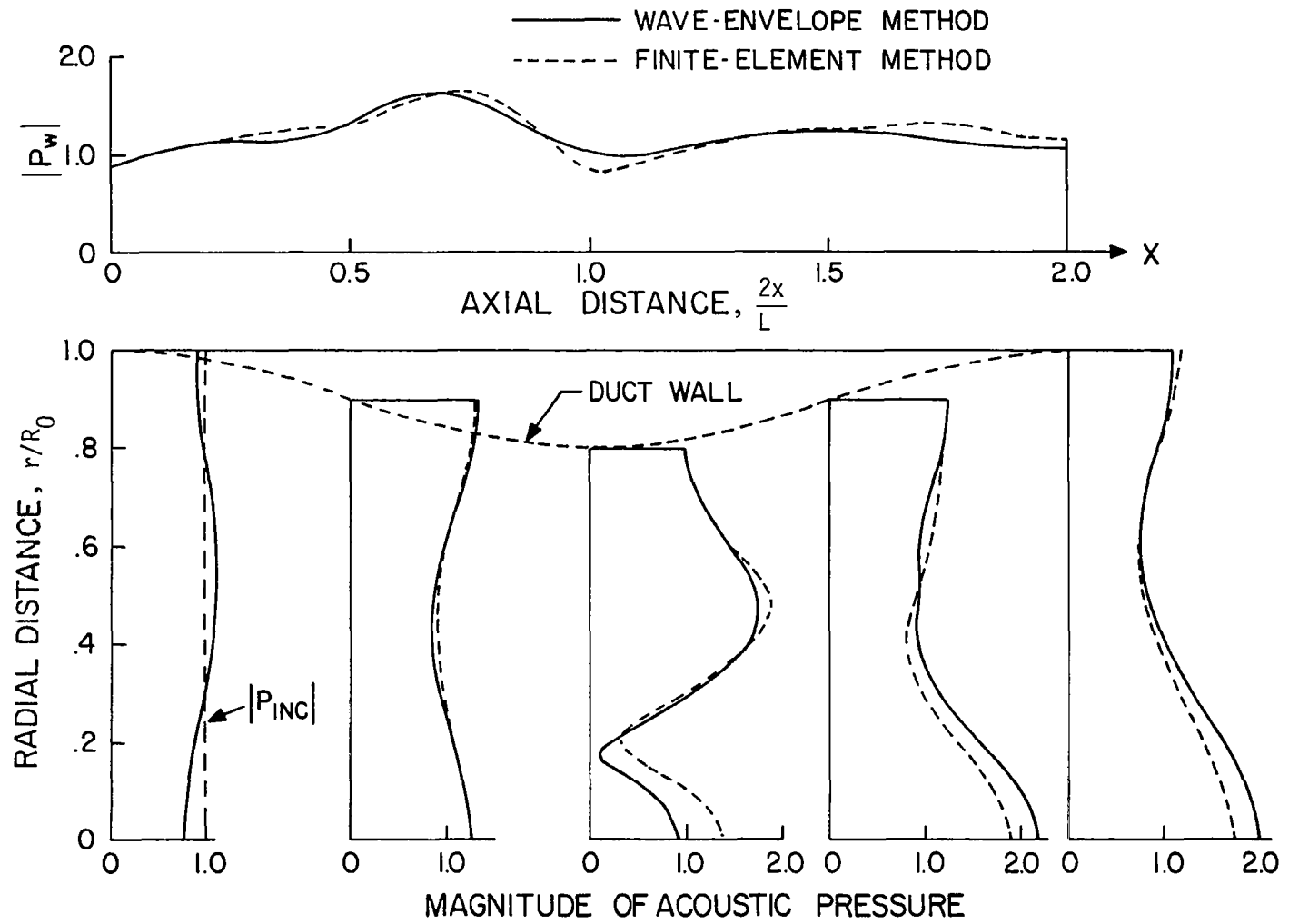


Figure 5. Comparison of wave-envelope and finite-element methods.

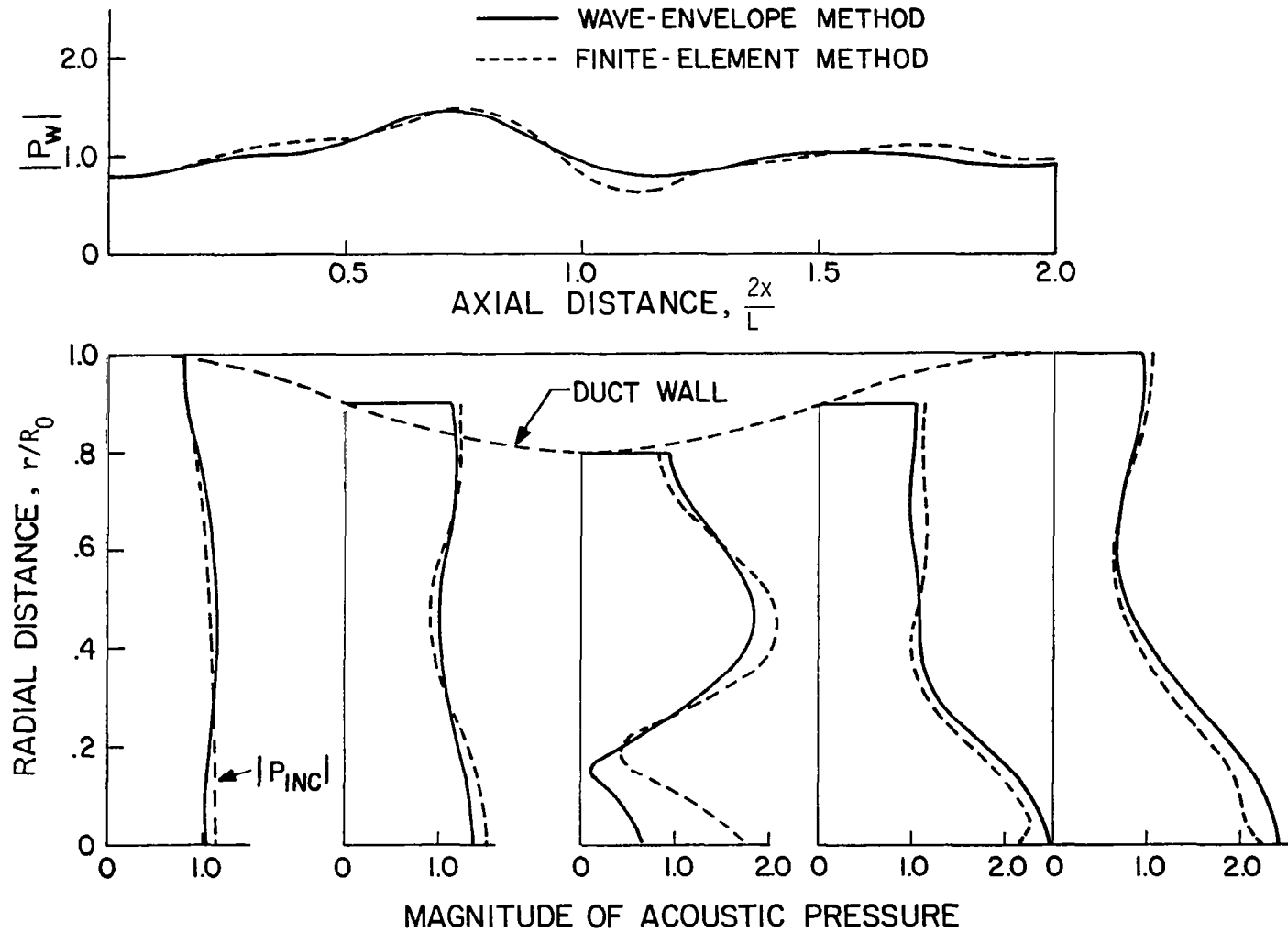


Figure 6. Comparison of wave-envelope and finite-element methods.

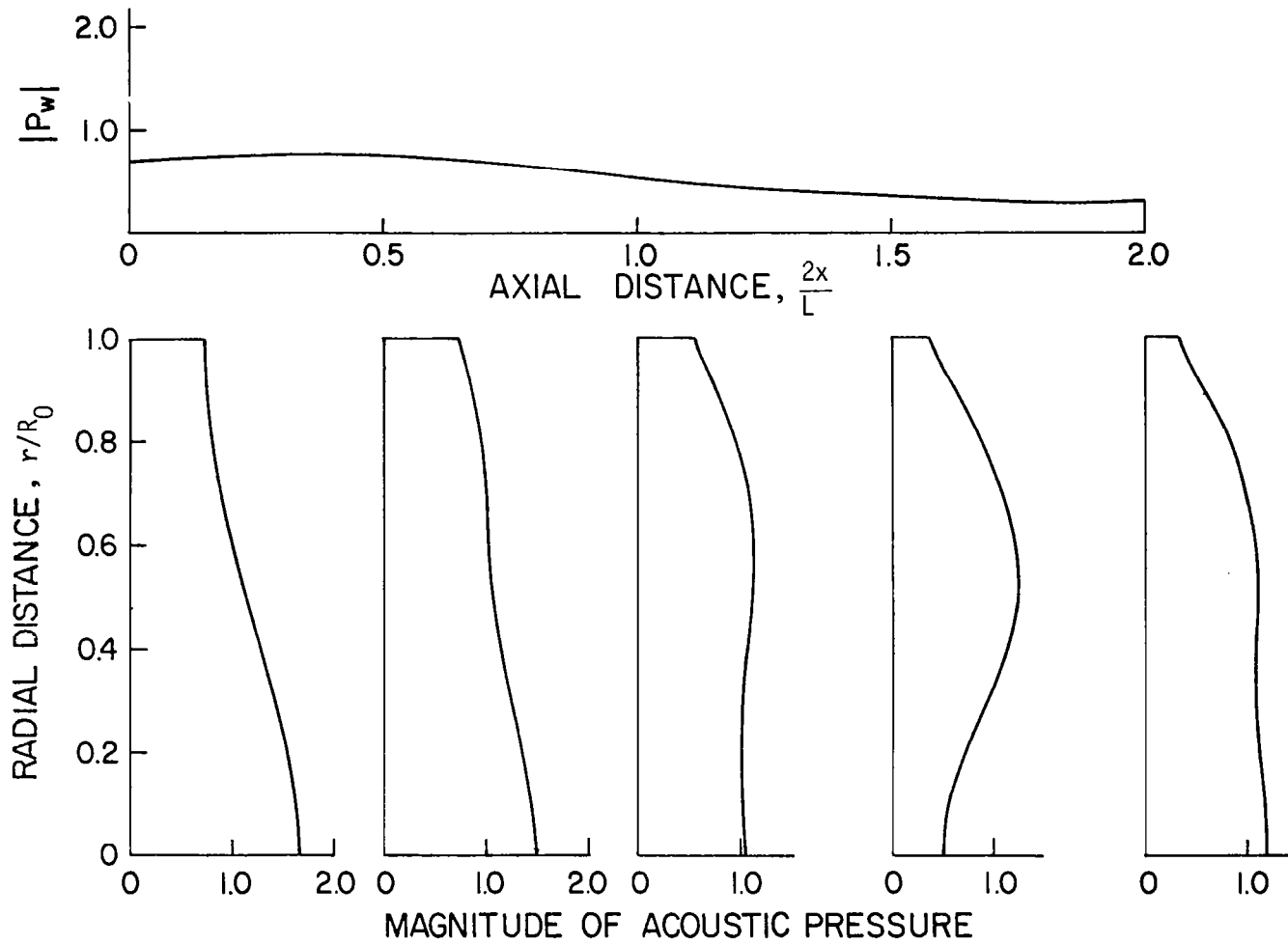


Figure 7. Variation of the acoustic pressure profiles with axial distance for a variable admittance and  $\omega = 9.12$ .

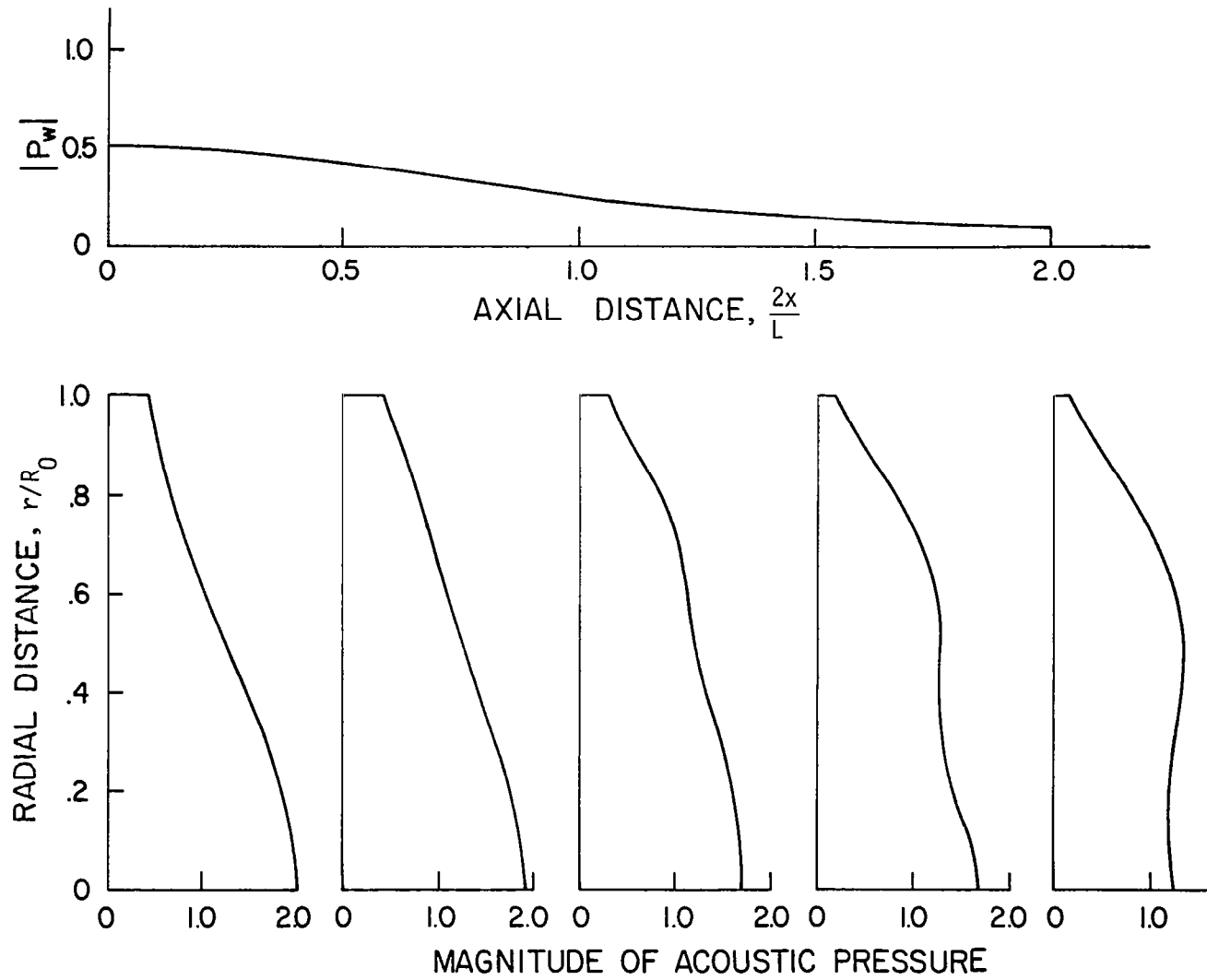


Figure 8. Variation of the acoustic pressure profiles with axial distance for a variable admittance and  $\omega = 18.24$ .

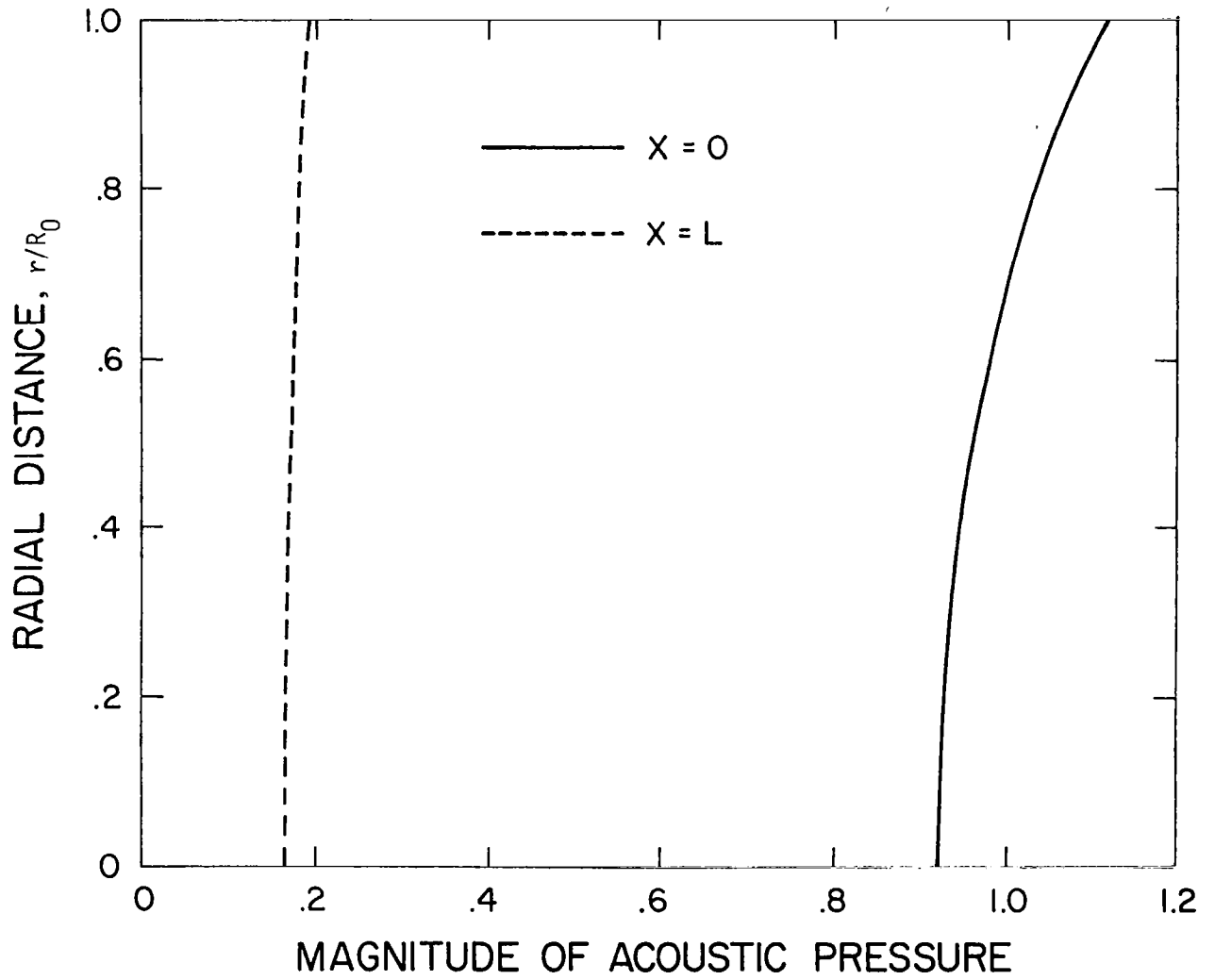


Figure 9. Comparison of the acoustic pressure profiles at two axial locations for a general axisymmetric case.

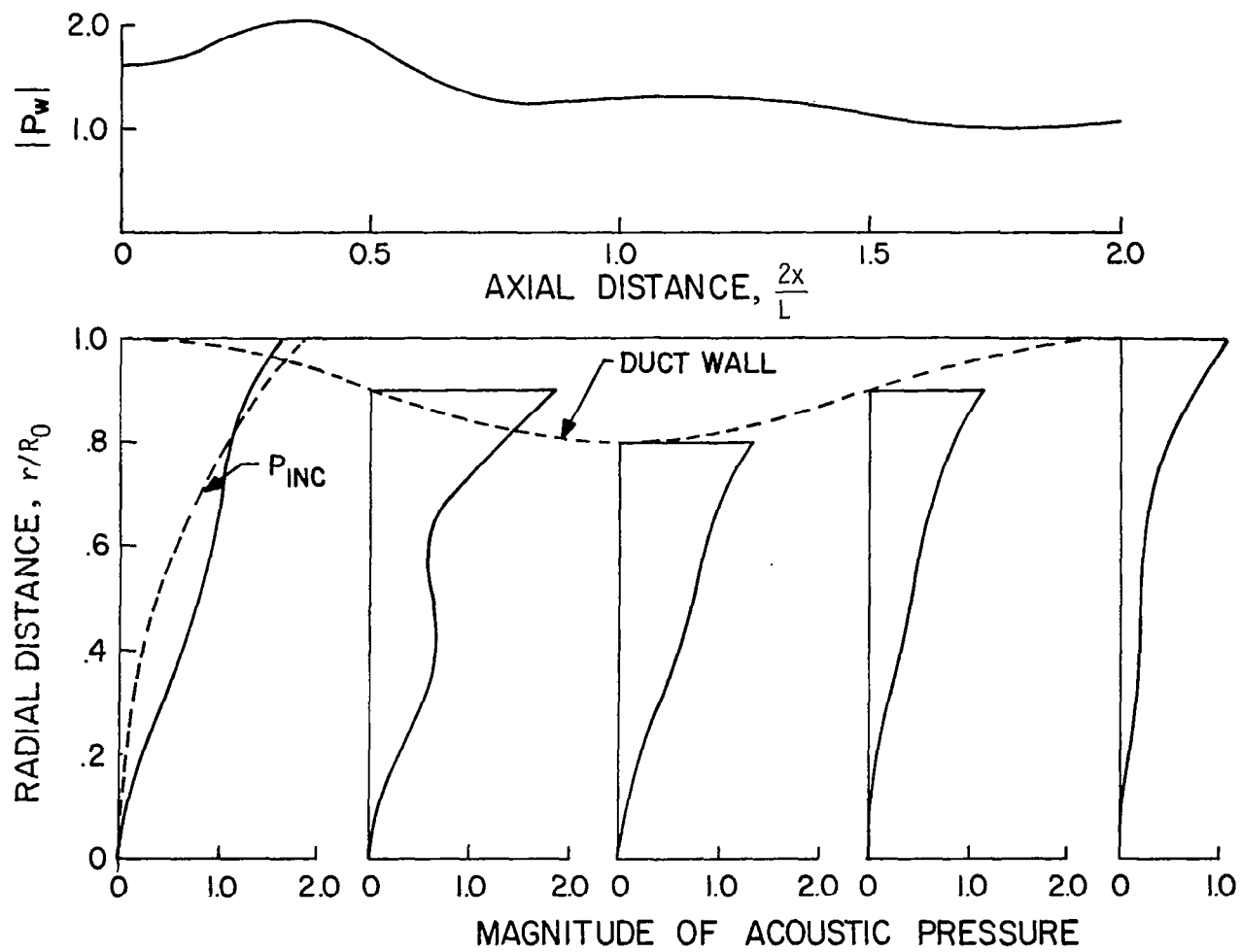


Figure 10. Variation of the acoustic pressure profiles with axial distance for a spinning mode case.

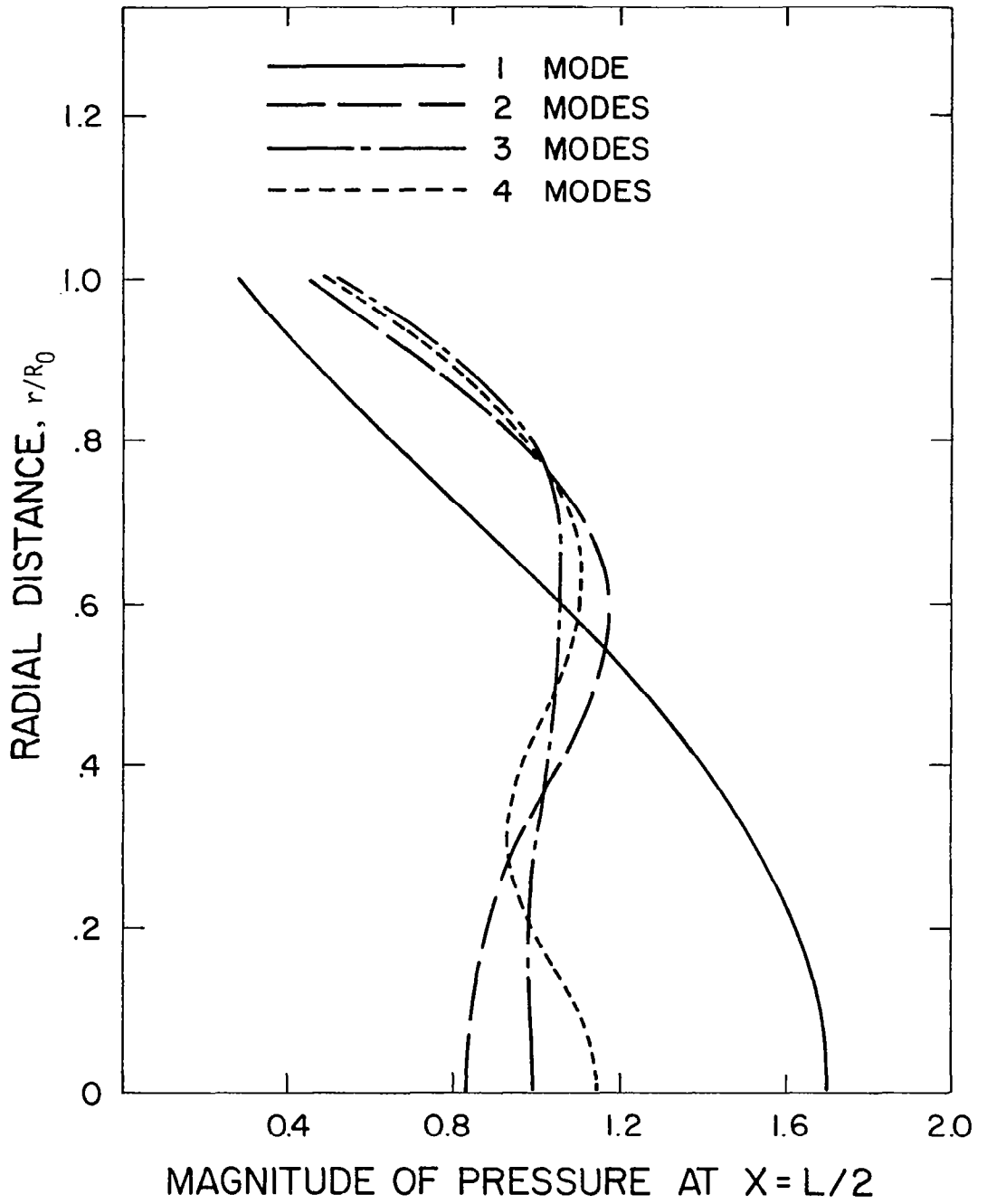


Figure 11a. Effect of increasing the number of modes on the convergence of the acoustic pressure profiles at the throat.

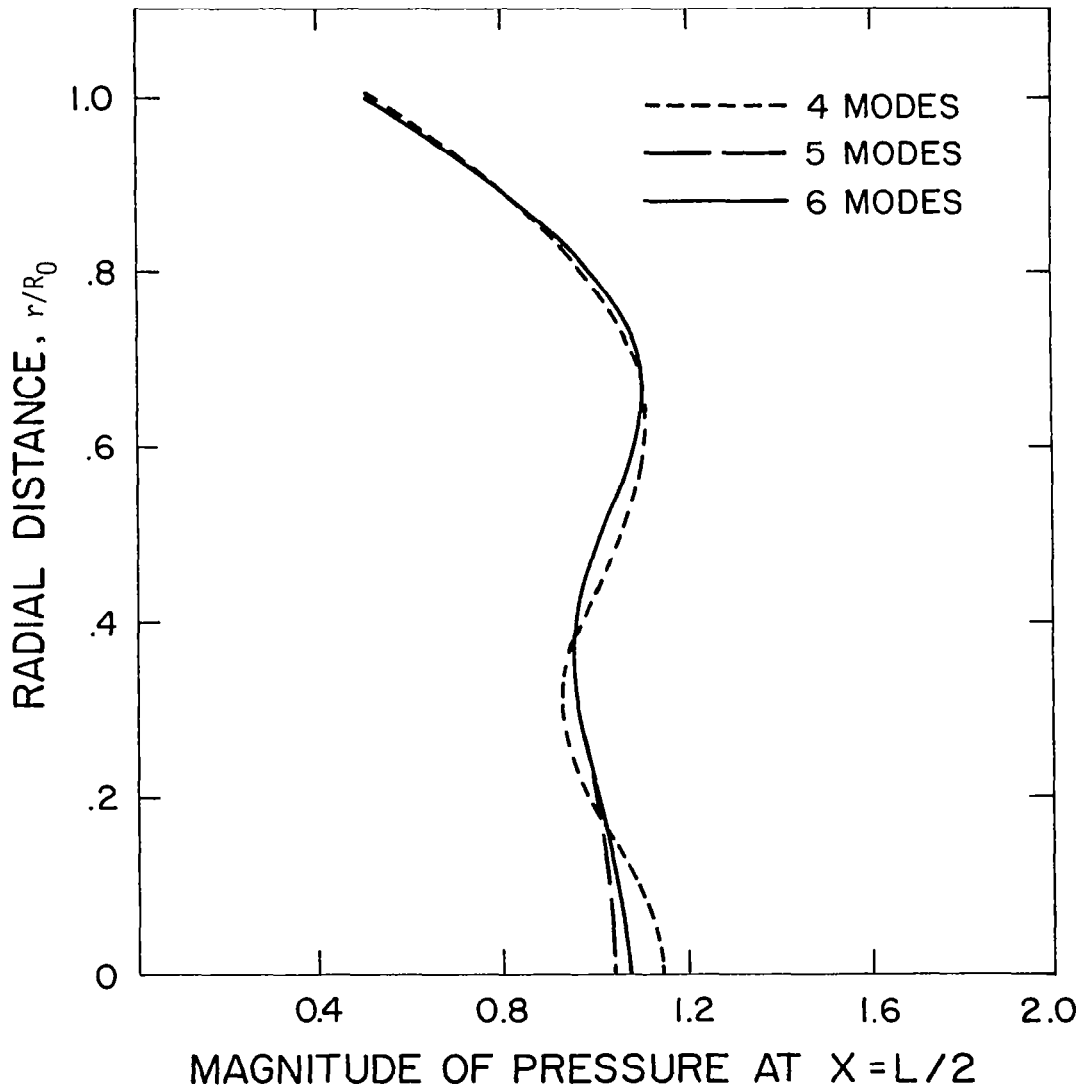


Figure 11b. Effect of increasing the number of modes on the convergence of the acoustic pressure profiles at the throat.

## REFERENCES

1. Myers, M. K. and Callegari, A. J., "On the Singular Behavior of Linear Acoustic Theory in Near-Sonic Duct Flows", *Journal of Sound and Vibration*, Vol. 51, pp. 517-531, 1977.
2. Nayfeh, A. H., Shaker, B. S., and Kaiser, J. E., "Computation of Nonlinear One-Dimensional Waves in Near-Sonic Flows", *AIAA Journal*, Vol. 16, pp. 1154-1159, 1978.
3. Lumsdaine, E., "Development of a Sonic Inlet for Jet Aircraft", *Internoise 1972 Proceedings*, pp. 501-506, 1972.
4. Klujber, F., Bosch, K. C., Demetrick, S. R. and Robb, W. R., "Investigation of Noise Suppression by Sonic Inlets for Turbofan Engines", Boeing Document D6-40855, NASA CR-121126, CR-121127, July, 1973.
5. Sobel, J. A. and Welliver, A. D., "Sonic Block Silencing for Axial and Screw-Type Compressor", *Noise Control*, Vol. 7, No. 5, pp. 9-11, Sept/Oct., 1961.
6. Greatrex, F. B., "By-Pass Engine Noise", *Trans. SAE*, Vol. 69, pp. 312-324, 1961.
7. Sawhill, R. H., "Investigation of Inlet Airflow Choking as a Mean of Suppressing Compressor Noise - 5' Inlet Model", Boeing Documents D6A-10155-1, 1966.
8. Cawthorne, J. M., Morris, G. J., and Hayes, C., "Measurement of Performance, Inlet Flow Characteristics, and Radiated Noise for a Turbojet Engine Having Choked Inlet Flow", NASA TN D-3929, 1967.
9. Anderson, A. O., "An Acoustic Evaluation on the Effect of Choking using a Modal Supersonic Inlet", Boeing Document D6A-10378-1, 1966.
10. Anderson, R., Destafanis, P., Farguhar, B. W., Giarda, G., Shuehle, A., and Van Duine, A. A., "Boeing/Aeritalia Sonic Inlet Feasibility Study", Boeing Document D6-40208, 1972.
11. Chestnutt, D. and Stewart, N. D., "Axial Flow Compressor Noise Reduction by Means of Inlet Guide Van Choking", NASA Langley Working Paper, LWP-473, Nov. 1967.

12. Chestnutt, D., "Noise Reduction by Means of Inlet-Guide-Vane Choking in an Axial-Flow Compressor", NASA TN D-4682, 1968.
13. Hawking, D. L. and Lawson, M. V., "Theoretical Investigation of Supersonic Rotor Noise", Loughborough University Report TT7213, Dec. 1972.
14. Benzakein, M. J., Kazin, S. B. and Savell, C. T., "Multiple Pure-Tone Noise Generation and Control", AIAA Paper No. 73-1021, October 1973.
15. Klujber, F., "Results of an Experimental Program for the Development of Sonic Inlets for Turbofan Engines", AIAA Paper No. 73-222.
16. Higgins, C. C., Smith, J. N., and Wise, W. H., "Sonic Throat Inlets", NASA SP-189, pp. 197-215, 1968.
17. Koch, R. L., Ciskowski, T. M., and Garzon, J. R., "Turbofan Noise Reduction Using a Near Sonic Inlet", AIAA Paper No. 74-1098, 1974.
18. Miller, B. A. and Abbott, J. M., "Aerodynamic and Acoustic Performance of Two Choked Flow Inlets under Static Condition", NASA-TM-X-2629-E7008.
19. Abbott, J. M., "Aeroacoustic Performance of Scale Model Sonic Inlets - Takeoff/Air Approach Noise Reduction", AIAA Paper No. 74-202, 1975.
20. Groth, H. W., "Sonic Inlet Noise Attenuation and Performance with a J-85 Turbojet Engine as a Noise Source", AIAA Paper No. 74-91, 1974.
21. Savkar, S. D. and Kazin, S. B., "Some Aspects of Fan Noise Suppression Using High Mach Number Inlets", AIAA Paper No. 74-554, 1974.
22. Miller, B. A., "Experimentally Determined Aeroacoustic Performance and Control of Several Sonic Inlets", AIAA Paper No. 75-1184, 1975.
23. Chestnutt, D. and Clark, L. R., "Noise Reduction by Means of Variable-Geometry Inlet Guide Vanes in a Cascade Apparatus" NASA TM X-2392, 1971.
24. Nayfeh, A. H., Kaiser, J.E., and Telionis, D. P., "Acoustics of Aircraft Engine-Duct Systems", AIAA Journal, Vol. 13, pp. 130-153, 1975.

25. Nayfeh, A. H., "Sound Propagation Through Nonuniform Ducts", Proceedings of the Society of Engineering Science at NASA Langley Research Center, November 1-3, 1976.
26. Vaidya, P. G., and Dean, P. D., "State of the Art of Duct Acoustics", AIAA Paper No. 77-1279.
27. Webster, A. G., "Acoustical Impedance and the Theory of Horns and of the Phonograph", Proceedings of the National Academy of Science, Vol. 5, pp. 275-282, 1919.
28. Stevenson, A. F., "Exact and Approximate Equations for Wave Propagation in Acoustic Horns", Journal of Applied Physics, Vol. 22, pp. 1461-1463, 1951.
29. Eversman, W., Cook, E. L., and Beckemeyer, R. J., "A Method of Weighted Residuals for the Investigation of Sound Transmission in Non-Uniform Ducts with Flow", Journal of Sound and Vibration, Vol. 38, pp. 105-123, 1975.
30. Alfredson, R. J., "The Propagation of Sound in a Circular Duct of Continuously Varying Cross-Sectional Area", Journal of Sound and Vibration, Vol. 23, 1972.
31. Nayfeh, A. H. and Telionis, D. P., "Acoustic Propagation in Ducts with Varying Cross-Sections", Journal of the Acoustical Society of America, Vol. 54, No. 6, pp. 1654-1661, 1973.
32. Nayfeh, A. H., Perturbation Methods, Wiley-Interscience, New York, Chapter 6, 1973.
33. Isakovitch, M. A., "Scattering of Sound Waves on Small Irregularities in a Wave Guide", Akusticheskii Zhurnal, Vol. 3, 1957.
34. Samuels, J. S., "On Propagation of Waves in Slightly Rough Ducts", The Journal of the Acoustical Society of America, Vol. 31, March 1959, pp. 319-325.
35. Saïant, R. F., "Acoustic Propagation in Waveguides with Sinusoidal Walls", The Journal of the Acoustical Society of America, Vol. 53, Feb. 1973, pp. 504-507.
36. Nayfeh, A. H., "Sound Waves in Two-Dimensional Ducts with Sinusoidal Walls", Journal of the Acoustical Society of America, Vol. 56, pp. 768-770, 1974.

37. Nayfeh, A. H., "Acoustic Waves in Ducts with Sinusoidally Perturbed Walls and Mean Flow", *Journal of the Acoustical Society of America*, Vol. 57, pp. 1036-1039, 1975.
38. Nayfeh, A. H., and Kandil, O. A., "Propagation of Waves in Cylindrical Hard-Walled Ducts with General Weak Undulations", *AIAA Journal*, Vol. 16, pp. 1041-1045, 1978.
39. Quinn, D. W., "A Finite Difference Method for Computing Sound Propagation in Nonuniform Ducts", *AIAA Paper No. 75-130*, 1975.
40. Baumeister, K. J. and Rice, E. J., "A Difference Theory for Noise Propagation in an Acoustically Lined Duct with Mean Flow", *Progress in Astronautics and Aeronautics*, Vol 37, *Aeroacoustic*, pp. 435-453, ed., H. T. Nagamatsu, MIT Press, 1975.
41. Baumeister, K. J., "Wave Envelope Analysis of Sound Propagation in Ducts with Variable Axial Impedance", *Progress in Astronautics and Aeronautics*, Vol. 44, *Aeroacoustics*, pp. 451-474, ed. I.R. Schwartz, MIT Press, 1976.
42. Powell, A., "Theory of Sound Propagation through Ducts Carrying High-Speed Flows", *Journal of the Acoustical Society of America*, Vol. 32, pp. 1640-1646, 1960.
43. Eisenberg, N. A. and Kao, T. W., "Propagation of Sound Through a Variable-Area Duct with a Steady Compressible Flow", *Journal of the Acoustical Society of America*, Vol. 49, pp. 169-175, 1971.
44. Davis, S. S. and Johnson, M. L., "Propagation of Plane Waves in a Variable Area Duct Carrying a Compressible Subsonic Flow", presented at the 87th Meeting of the Acoustical Society of America, New York, 1974.
45. Huerre, P. and Karamcheti, K., "Propagation of Sound through a Fluid Moving in a Duct of Varying Area", in *Interagency Symposium of University Research in Transportation Noise*, Stanford, Vol. II, pp. 397-413, 1973.
46. King, L. S. and Karamcheti, K., "Propagation of Plane Waves in the Flow Through a Variable Area Duct", *Progress in Astronautics and Aeronautics*, Vol. 37, *Aeroacoustics*, pp. 403-418, ed. H. T. Nagamatsu, MIT Press, 1975.

47. Nayfeh, A. H., Telionis, D. P., and Lekoudis, S. G., "Acoustic Propagation in Ducts with Varying Cross Sections and Sheared Mean Flow", Progress in Astronautics and Aeronautics, Vol. 37, Aeroacoustics, pp. 333-351, ed. H. T. Nagamatsu, MIT Press, 1975.
48. Nayfeh, A. H., Kaiser, J. E., and Telionis, D. P., "Transmission of Sound Through Annular Ducts of Varying Cross Sections", AIAA Journal, Vol. 13, No. 1, pp. 60-65, 1975.
49. Nayfeh, A. H., Kaiser, J. E., "Effect of Compressible Sheared Mean Flow on Sound Transmission Through Variable-Area Plane Ducts", AIAA Paper 75-128, 1975.
50. Nayfeh, A. H., Kaiser, J. E., Marshall, R. L., and Hurst, C. J., "An Analytical and Experimental Study of Sound propagation and Attenuation in Variable-Area Ducts", NASA CR-135342, 1978.
51. Eversman, W., "A Multimodal Solution for the Transmission of Sound in Nonuniform Hard Wall Ducts with High Subsonic Flow" AIAA Paper No. 76-497, 1976.
52. Nayfeh, A. H., Shaker, B. S., and Kaiser, J. E., "Transmission of Sound Through Nonuniform Circular Ducts with Compressible Mean Flows", NASA CR-145126, V.P.I.&SU, Blacksburg, Va., May 1977.
53. Sigman, R. K., Majjigi, R. K., and Zinn, B. T., "Determination of Turbofan Inlet Acoustics Using Finite Elements," AIAA Journal, Vol. 16, 1139-1145, 1978.
54. Abrahamson, A. L., "A Finite Element Algorithm for Sound Propagation in Axisymmetric Ducts Containing Compressible Mean Flow", NASA CR-145209, Wylie Laboratories, Hampton, Va., June 1977; also: "A Finite Element Model of Sound Propagation in a Non-Uniform Circular Duct Containing Compressible Flow", AIAA Paper 77-1301, 1977.
55. Kaiser, J. and Nayfeh, A. H., "A Wave-Envelope Technique for Wave Propagation in Nonuniform Ducts", AIAA Journal, Vol. 15, No. 4, pp. 533-537, April 1977.
56. Schlichting, H., Boundary-Layer Theory, 6th Ed., McGraw-Hill, New York, pp. 61 and 254, 1968.
57. Nayfeh, A. H., "Effect of the Acoustic Boundary Layer on the Wave Propagation in Ducts", Journal of the Acoustical Society of America, Vol. 54, No. 6, pp. 1737-1742, Dec. 1973.

58. Pestorius, F. M., and Blackstock, D. T., "Nonlinear Distortion in the Propagation of Intense Acoustic Noise", Interagency Symposium on University Research in Transportation Noise Proceedings, Vol. II. pp. 565-577, 1973.
59. Zorumski, W. E., "Acoustic Theory of Axisymmetric Multisectioned Ducts", NASA TR R-419, May 1974.
60. Nayfeh, A. H. and Sun, J., "Effect of Transverse Velocity and Temperature Gradients on Sound Attenuation in Rectangular Ducts", Journal of Sound and Vibration, Vol. 34, No. 4, pp. 505-517, June 1974.
61. Nayfeh, A. H., Kaiser, J. E., and Shaker, B. S., "Effect of Mean-Velocity Profile Shapes on Sound Transmission Through Rectangular Ducts", Journal of Sound and Vibration, Vol. 34, No. 3, pp. 413-423, June 1974.
62. Hersh, A. S., and Catton, I., "Effect of Shear Flow on Sound Propagation in Rectangular Ducts", The Journal of Acoustical Society of America, Vol. 50, No. 3, pp. 992-1003, Sept. 1971.
63. Unruh, J. F. and Eversman, W., "The Utility of the Galerkin Method for the Acoustic Transmission in an Attenuating Duct", Journal of Sound and Vibration, Vol. 23, No. 2, pp. 187-197, July 1972.
64. Morfey, C. L., "Acoustic Energy in Non-Uniform Flows", Journal of Sound and Vibration, Vol. 14, No. 2, pp. 159-170, 1971.
65. Eversman, W., "Energy Flow Criteria for Acoustic Propagation in Ducts with Flow", Journal of the Acoustical Society of America, Vol. 49, No. 6, pp. 1717-1721, June 1971.
66. Möhring, W., "Energy Flux in Duct Flow", Journal of Sound and Vibration, Vol. 18, No. 1, pp. 101-109, 1971.

1. Report No. NASA CR-3109		2. Government Accession No.		3. Recipient's Catalog No.	
4. Title and Subtitle A Wave-Envelope Analysis of Sound Propagation in Nonuniform Circular Ducts with Compressible Mean Flows				5. Report Date March 1979	
				6. Performing Organization Code	
7. Author(s) A. H. Nayfeh, J. E. Kaiser, and B. S. Shaker				8. Performing Organization Report No.	
9. Performing Organization Name and Address Virginia Polytechnic Institute and State University Department of Engineering Science and Mechanics Blacksburg, Virginia 24061				10. Work Unit No. 505-03-13-12	
				11. Contract or Grant No. NAS1-13884	
12. Sponsoring Agency Name and Address National Aeronautics and Space Administration Washington, DC 20546				13. Type of Report and Period Covered Contractor Report	
				14. Sponsoring Agency Code	
15. Supplementary Notes Langley Technical Monitor: Joe W. Posey Final Report					
16. Abstract An acoustic theory is developed to determine the sound transmission and attenuation through an infinite, hard-walled or lined circular duct carrying compressible, sheared, mean flows and having a variable cross section. The theory is applicable to large as well as small axial variations, as long as the mean flow does not separate. The technique is based on solving for the envelopes of the quasi-parallel acoustic modes that exist in the duct instead of solving for the actual wave, thereby reducing the computation time and the round-off error encountered in purely numerical techniques. The solution recovers the solution based on the method of multiple scales for slowly varying duct geometry.  A computer program has been developed based on the wave-envelope analysis for general mean flows. The mean-flow model consists of a one-dimensional flow in an inviscid core and a quarter-sine profile in the boundary layer. Mean radial velocity effects can be included. Results are presented for the reflection and transmission coefficients as well as the acoustic pressure distributions for a number of conditions: both straight and variable area ducts with and without liners and mean flows from very low to high subsonic speeds are considered. A number of test cases that demonstrate the flexibility of the program are included.					
17. Key Words (Suggested by Author(s)) Duct Acoustics Variable Area Ducts Sound Propagation			18. Distribution Statement Unclassified - Unlimited  Subject Category 71		
19. Security Classif. (of this report) Unclassified		20. Security Classif. (of this page) Unclassified		21. No. of Pages 67	22. Price* \$5.25

\* For sale by the National Technical Information Service, Springfield, Virginia 22161

NASA-Langley, 1979